J. Physiol. (1974), **239**, *pp.* 393-434
With 20 text-figures
Printed in Great Britain

KINETICS AND STEADY-STATE PROPERTIES OF THE CHARGED SYSTEM CONTROLLING SODIUM CONDUCTANCE IN THE SQUID GIANT AXON

BY R. D. KEYNES* AND E. ROJAS

From the Laboratory of the Marine Biological Association, Plymouth, the Laboratorio de Fisiologia Celular, Universidad de Chile, Casilla 657, Viña del Mar, Chile and the Agricultural Research Council Institute of Animal Physiology, Babraham, Cambridge

(*Received 14 December 1973*)

SUMMARY

1. Asymmetries in the early time course of the displacement current passing across the membrane after application of equal voltage-clamp pulses in the two directions have been investigated in the squid giant axon. Before making the measurements, Na current was blocked by removal of external Na and treatment with tetrodotoxin. Potassium current was usually blocked by perfusion with CsF, but some experiments were done with intact axons. A signal averaging technique was used to eliminate the symmetrical components of the membrane current.

2. The asymmetrical current had a contribution of appreciable size attributed to the movement of mobile charges or dipoles in the membrane. This was manifested as an outward current rising rapidly to a peak on depolarization of the membrane and then declining exponentially to zero, followed at the end of the pulse by an inward surge of current with a similar time course. There was also a sustained flow of current outwards during the pulse, arising from ionic leakage with a rectifying characteristic.

3. The identification of the exponentially changing current component with the displacement of charged particles forming an integral part of the membrane was supported by the demonstration that the total transfer of charge was equal and opposite at the beginning and end of the pulse, that it reached saturation when the internal potential was taken to a sufficient positive value, and that its size was unaffected by temperature, although its time constant had a large temperature coefficient.

4. The disposition of the mobile charges in the steady state was shown to obey a Boltzmann distribution. At the midpoint of the distribution curve, the proportion of the charge displaced underwent an e-fold change for a

* Present address: Physiological Laboratory, Cambridge CB2 3EG.

19 mV change in potential. The effective valency of the particles, that is their actual charge multiplied by the fraction of the electric field acting on them, was therefore 1·3.

5. The total quantity of mobile charge was estimated as about 1500×10^{-12} C for 0·05 cm^2 of membrane, corresponding to some 1900 charges/μm^2.

6. The identification of these mobile charges with the gating particles responsible for controlling Na conductance was supported by the findings that (*a*) their time constants were the same as those of Hodgkin & Huxley's '*m*' system, both in absolute magnitude and in their dependence on potential and temperature, (*b*) the transition potential at which the charges were evenly distributed on the two sides of the membrane also agreed with that for the '*m*' system in intact axons, and its value was similarly shifted in a positive direction by a reduction in internal ionic strength or by raising the external Ca concentration, (*c*) comparison of the steepness of the curves governing on the one hand the steady-state distribution of the mobile charges and on the other the Na conductance, suggested that an effective cooperation of the charges in groups of three was involved, again in excellent agreement with the '*m*' system.

7. Displacement of the mobile charges was unaffected by external pH over the range 5–8, but preliminary observations showed that 1 % procaine reduced the total charge transfer to somewhat less than 40 % of the initial value, and roughly halved the time constant.

INTRODUCTION

It is implicit in Hodgkin & Huxley's (1952) description of the changes in ionic permeability underlying excitation and conduction in nerve that the mechanism depends fundamentally on the effect of the electric field on the distribution or orientation of membrane molecules with a charge or dipole moment. When, therefore, the membrane is depolarized, the passage of ionic current must be preceded not only by the surge of capacity current, but also by what has come to be known as the 'gating current', corresponding to the movement of these charged controlling particles in the membrane. However, Hodgkin & Huxley found no direct evidence for the existence of the gating current, and concluded that its contribution amounted to no more than a few per cent of the maximum ionic current, because many ions cross the membrane through each open channel.

The first attempt to investigate the question experimentally was made by Chandler & Meves (1965), who also were unable to identify any component of the membrane current with the operation of the gating mechanism, even when the ionic current had first been greatly reduced by removal of external Na and perfusion with a low ionic strength solution. They

estimated that the total charge carried by the gating particles was less than 10^{-8} C/cm^2, which fitted with the sparse distribution of tetrodotoxin binding sites in lobster leg nerve reported by Moore, Narahashi & Shaw (1967).

Once more using perfused squid axons in a Na-free solution, but blocking the Na channels with tetrodotoxin and employing a signal averager with voltage-clamp pulses of alternating polarity to eliminate symmetrical capacity current, Armstrong & Bezanilla (1973) have recently succeeded in recording a component of the membrane current with the main characteristics expected for the gating current. Adopting a very similar technique, we were able to extend their findings in several respects (Keynes & Rojas, 1973) and now present a more detailed account of our experiments.

METHODS

The experiments were performed with giant axons 500–900 μm in diameter dissected from the hindmost stellar nerve in mantles from *Loligo forbesi* or *L. vulgaris*. Generally the mantles had been stored for a few hours in ice-cold sea water before dissection, but sometimes living specimens were available. Most of the axons were perfused intracellularly and their membrane potential was controlled by the methods described by Rojas, Taylor, Atwater & Bezanilla (1969). Some of them were mounted intact in the same chamber, with an axial 100 μm Pt wire coated with Pt black inserted longitudinally through a cut at one end to carry the applied current, and the electrode bridge to record the internal potential similarly inserted from the opposite end.

The point control system for voltage-clamping developed by Moore & Cole (1963) was used in the form described by Bezanilla, Rojas & Taylor (1970). The voltage electrodes were Ag/AgCl. The internal electrode bridge was the usual glass capillary, about 200 mm in length and 100 μm in diameter, filled with 500 mM-KCl and containing a floating 50 μm bright Pt wire. The external electrode bridge was a length of polyethylene tubing filled with 1 % agar in 500 mM-Tris Cl. The external current electrode consisted of a pair of Pt plates coated with Pt black which were connected electrically and kept at virtual ground potential by means of the operational amplifier number 1 in Fig. 1. Two further pairs of Pt plates were used as guards on either side of the external current electrodes. The width of the external current electrodes was 2·5 mm, so that for a 750 μm axon the area of membrane from which current was collected was 0·059 cm^2.

Averaging technique

A block diagram of the arrangement of amplifiers for recording membrane current under membrane potential control is given in Fig. 1. The external current electrodes were kept at virtual ground potential by means of operational amplifier 1, and a current of 1 μA was thus converted into a voltage of 50 μV. Amplifier 2 had a voltage gain of 50, and amplifier 3 was the vertical amplifier of a 502 A Tektronix oscilloscope used with DC coupling and a gain setting of 20 mV/cm to give a gain of 100. The output of amplifier 3 was directly connected via a field effect transistor series-shunt switching circuit to an analogue signal averager, which was a Princeton Waveform Eductor Type TDH-9. The output of the signal averager was monitored on one beam of a 465 Tektronix oscilloscope with a 3A3 plug-in amplifier.

The mode of operation of this type of signal averager is as follows. A signal consisting of a repetitive waveform of interest together with unwanted noise is applied to the input; after amplification, this signal passes through a resistor to a set of 100 integrators or memory capacitors. Each capacitor has one end electrically connected to ground, and the other, by way of a series-insulated gate, to the signal. During each sweep, the gates open consecutively so that each of the memory capacitors is tied in turn to the signal for an equal interval. If the sweeps are synchronized with the repetitive wave form, the same portion of the wave form will

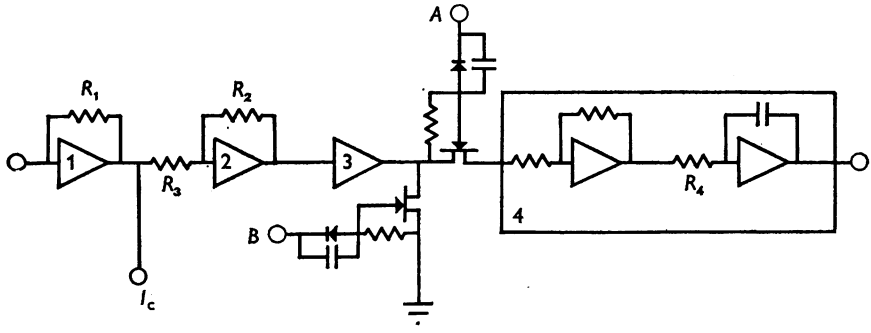

Fig. 1. Arrangement of current amplifiers. Amplifiers 1 and 2 were Philbrick P-45A, and 3 was the vertical amplifier of a Tektronix 502A oscilloscope. The signal averager is represented as 4. R_1 was 50 Ω, R_2 was 100,000 Ω, R_3 was 2,000 Ω. R_4 determined the characteristic time constant of the signal averager, and was generally 10,000 Ω. At the beginning and end of the voltage-clamp pulses, 50 μsec blanking pulses simultaneously took the potential at A from +15 to −15 V, and the potential at B from −15 to +15 V. Voltage-clamp current was monitored at the point marked I_c, the other parts of the voltage-clamp circuit being exactly as shown in Fig. 2 of Bezanilla *et al.* (1970).

be applied to a given capacitor in successive sweeps, and it will gradually build up in the memory. While the potential accumulated across the memory capacitors is still rising linearly, the signal–noise ratio is improved by the square root of the number of sweeps stored. The levels to which the individual capacitors are finally charged are read off sequentially through a unity gain output channel. The output voltage (V_{out}) of the signal averager is hence a function of the gain (μ) of its input amplifier, the total interval under analysis during each sweep (ΔT), the number of sweeps analysed (n), the size of the memory capacitors (C), the charging resistance (R_4), and the input voltage (V_{in}). If V_{in} is the average input signal over the time interval $\delta t = t_k - t_{k-1}$, where $k = 1, 2, 3, \ldots, 99, 100$, then for the kth capacitor during one sweep

$$V_{out} = \frac{1}{R_4 C} \int_{t_{k-1}}^{t_k} \mu . V_{in} . dt$$

$$= \frac{\mu . \delta t . V_{in}}{R_4 C}.$$

After n sweeps, provided that n is not too large,

$$V_{out} = \frac{n . \mu . \delta t . V_{in}}{R_4 C},$$

and since $\delta t = \Delta T/100$,

$$V_{out} = \frac{n.\mu.\Delta T.V_{in}}{100R_4C} = \frac{n.\mu.\Delta T.V_{in}}{\text{C.T.C}}. \quad (1)$$

The memory capacitors were each 5 μF. For most of the experiments the resistor R_4 was chosen to be 10,000 Ω, so that the value of the characteristic time constant (C.T.C.) was 5 sec. In order to avoid overloading the signal input channel, μ was set at 2. With these settings, only 60 pulses were needed to achieve an acceptable signal–noise ratio, and eqn. (1) becomes

$$V_{out} = 24.\Delta T.V_{in}. \quad (2)$$

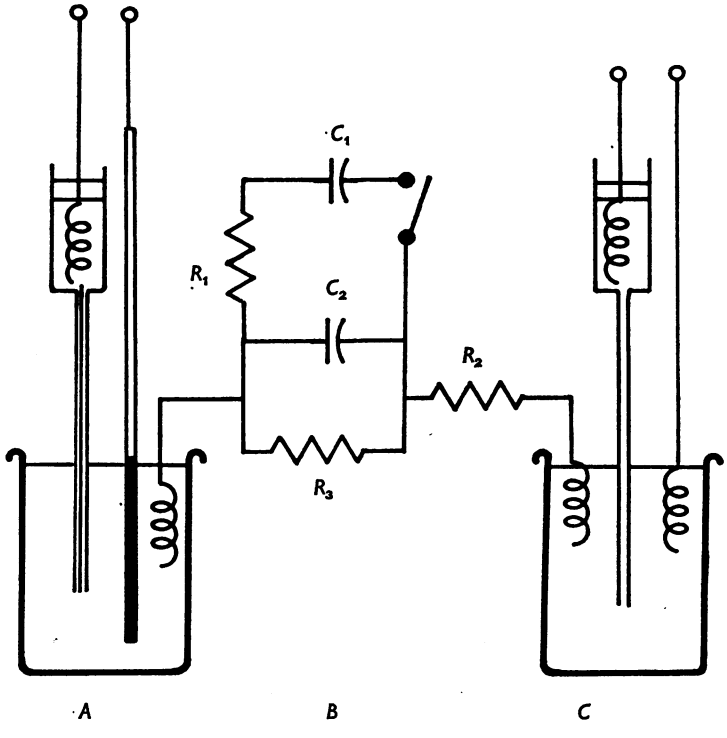

Fig. 2. Dummy circuit simulating an axon perfused with a low ionic strength solution. *A*. Beaker containing 55 mM-CsF plus sucrose, into which are dipped the internal voltage electrode and the axial Pt wire for application of current. *B*. Elements representing 0·05 cm² of membrane. C_2 was 0·05 μF, and since ΔI_L was about 3 μA for 120 mV pulses, R_3 was 40,000 Ω. The Schwann cell series resistance was taken as 4 Ω cm², so that R_2 was 80 Ω. A time constant of 150 μsec could be added in parallel as R_1C_1. C. Beaker containing Na- and Mg-free ASW, into which are dipped the external voltage and current electrodes. The rather large junction potential difference between the two solutions was backed off in the voltage-clamp circuit.

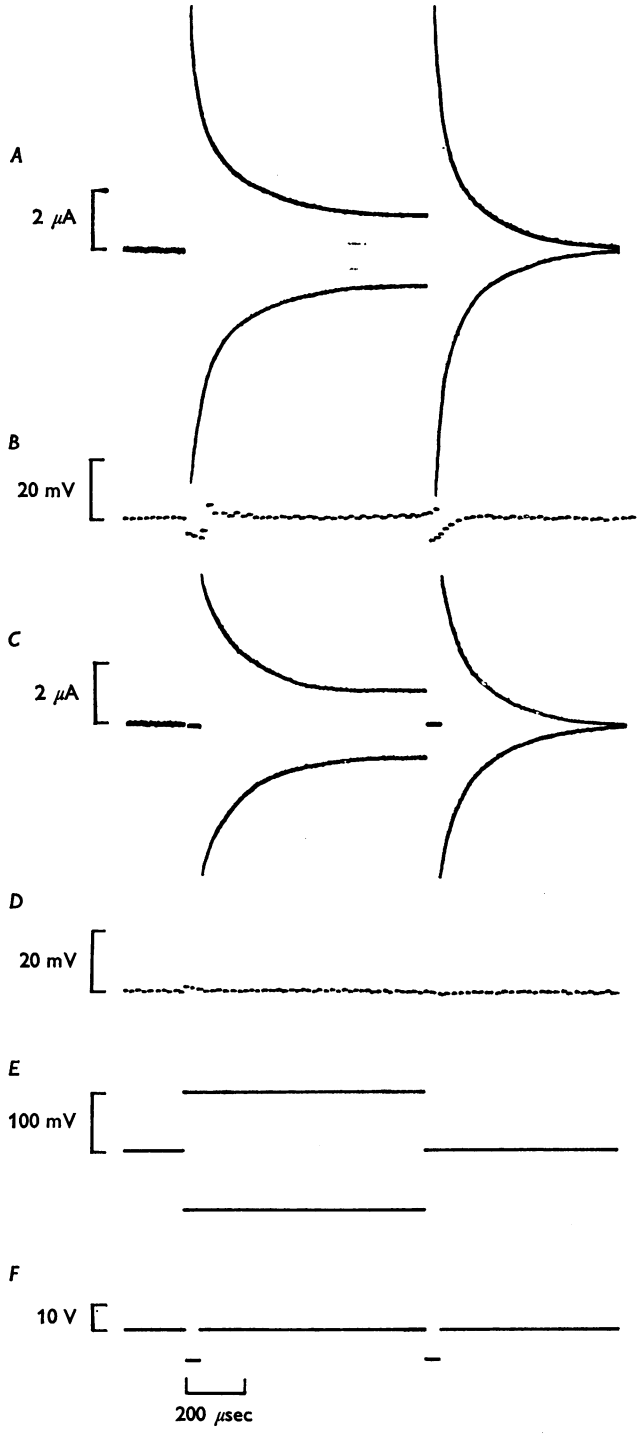

Fig. 3. For legend see facing page.

Gain and linearity of the recording system

In order to check the gain of the system, voltage-clamp pulses of known size were applied to a 10,000 Ω precision resistor, and the output of the signal averager when 60 pulses were summed was measured. A plot of V_{out} against pulse size was linear, obeying equation (2) with V_{in} = 250,000 × injected current in μA.

In order to test the performance of the system with a symmetrical capacity transient added to the injected current, the dummy shown in Fig. 2 was constructed. The resistances and capacitances in this dummy were of the same order of magnitude as those measured in axons internally perfused with solutions of low ionic strength. Pulses were applied to the dummy with the electrodes actually used in the experiments dipped into beakers representing the inner and outer sides of the axon membrane. Fig. 3*A* shows the transients at the input to the signal averager when voltage-clamp pulses of ± 100 mV (*E*) were applied. Record *B* shows the output read out after pulses had been applied for 60 sec at 2/sec, their polarity being changed at intervals of 5 sec; it may be seen that the signals accumulated at four or five of the individual addresses were out of line at the beginning and end of each pulse, indicating that there were slight departures from linearity at the peaks of the capacity transients. This potential source of error in measuring the asymmetrical components of the membrane current was almost completely eliminated (Fig. 3*D*) by applying the 50 μsec blanking pulses shown in Fig. 3*F* to the transistor switching circuit connected across the input to the signal averager. A similar switching arrangement was employed by Armstrong & Bezanilla (1973), but their 'window' was open only for a single period delayed 10–30 μsec after the beginning or end of the voltage-clamp pulse, so that records could not be made simultaneously for 'on' and for 'off'.

Solutions and experimental procedures

The composition of the solutions used is given in Table 1. All were prepared with double-glass-distilled water. Fluoride solutions were stored at 4° C in plastic containers.

As a normal routine, the axons were first bathed in K-free artificial sea water (K-free ASW) for a few minutes, and then internally perfused with CsF; but a few experiments were performed with intact axons that were not perfused. Sometimes a standard voltage-clamp run was conducted at this stage, and Table 2 gives various quantities that were then measured. Since internal perfusion with CsF almost completely blocks the outward membrane current through the K channels (Chandler & Meves 1970*a*), the inward currents observed in perfused axons were attributable exclusively to the Na system. In this connexion, it should be noted that throughout this paper all potentials will be referred to the external solution as ground, so that the resting membrane potential is negative. Potential changes in the positive direction which first reduce and then reverse the membrane potential are referred to as depolarizations; negative-going changes are hyperpolarizations.

Next, the external solution was replaced by one of the solutions containing neither Na nor K, but with 300 nM tetrodotoxin or saxitoxin. After 30 min exposure to the

Fig. 3. Controls of the performance of the current amplifiers and the signal averager. *A*. Transients at the input to the signal averager for the voltage-clamp pulses shown in *E*, with no blanking. *B*. Output of the signal averager after 60 pairs of pulses as in *A*. *C*. Transients at the input to the signal averager with the same voltage-clamp pulses but blanking as in *F*. *D*. Output of the signal averager after 60 pairs of pulses as in *C*.

TABLE 1. Composition of the solutions used for internal perfusion and bathing externally

A. Internal F solutions

	K^+ (mM)	Cs^+ (mM)	Tris Cl (mM)	Sucrose (mM)	pH
High K	550	—	10	—	7·3
Low K	275	—	10	500	7·1–7·3
High Cs	—	275	10	500	7·1–7·4
Low Cs	—	55	10	1000	7·1–7·3

B. External Cl solutions

	K^+ (mM)	Na^+ (mM)	Ca^{2+} (mM)	Mg^{2+} (mM)	$Tris^+$ (mM)	Isethionate (mM)	Toxin (nM)	pH
ASW	10	430	10	50	5	—	—	7·3–7·5
K-free ASW	—	430	10	50	15	—	—	7·3
Na and K-free saline	—	—	10	50	445	—	—	7·3
Na and K-free tetrodotoxin or saxitoxin saline	—	—	10	50	445	—	300	7·3
Na, K and Mg-free tetrodotoxin saline	—	—	10	—	595	—	300	7·3
High Ca tetrodotoxin saline	—	—	110	—	415	—	300	7·0–7·1
Isethionate saline	—	—	10	50	430	430	300	7·3

toxin at this concentration, the sodium channels could be assumed to be completely blocked (F. Bezanilla, R. D. Keynes, E. Rojas & R. E. Taylor, in preparation), and the axon was ready for observation of the gating currents. On completion of the gating current runs, the K-free ASW was reintroduced into the chamber, and 30–60 min were allowed for recovery before making a final set of voltage-clamp records from which the data given in Table 2 were derived. If the Na conductance was not restored to a reasonable value, the results were discarded, but in the majority of the experiments there was excellent recovery.

Although any residual junction potential difference between the internal and external voltage electrodes was always backed off at the beginning of each experiment, the subsequent solution changes and drifts in electrode potential could have altered the junction potential during the runs by an amount estimated in later tests as up to 10 mV. Hence there is a similar degree of uncertainty in our figures for the absolute value of the transition potential V'.

RESULTS

Direct measurement of asymmetries in voltage-clamp current records

Fig. 4*A* shows tracings of a typical pair of membrane current records obtained for an axon internally perfused with low ionic strength CsF

Expt. no.	Condition	Na conductance (1) (mmho/cm²)	Na conductance (2) (mmho/cm²)	K conductance (1) (mmho/cm²)	K conductance (2) (mmho/cm²)	Shift of $I-V$ curve (1) (mV)	Shift of $I-V$ curve (2) (mV)	Na reversal potential (1) (mV)	Na reversal potential (2) (mV)	Leakage current (1) (mA/cm²)	Leakage current (2) (mA/cm²)	Max. Na current (1) (mA/cm²)	Max. Na current (2) (mA/cm²)	Potential for e-fold change in G_{Na} (1) (mV)	Potential for e-fold change in G_{Na} (2) (mV)
21-D-1	Perfused *forbesi*	—	19	—	—	—	15	—	+74	—	0·05	—	1·4	—	—
1-J-3	Perfused *forbesi*	—	45	—	22	—	—	—	+55	—	0·09	—	2·3	—	—
4-J-2	Perfused *vulgaris**	—	38	—	—	—	—	—	+73	—	0·10	—	2·0	—	—
4-J-3	Intact *vulgaris**	—	60	—	—	—	—	—	+53	—	0·13	—	2·8	—	—
5-J-1	Intact *vulgaris**	—	17	—	31	—	—	—	+52	—	0·15	—	1·4	—	—
5-J-2	Intact *vulgaris**	—	74	—	50	—	12†	—	+54	—	0·07	—	3·5	—	—
8-J-2	Intact *forbesi*	79	55	62	60	—	—	+55	+54	0·06	0·07	3·9	3·0	7	6·5
9-J-1	Perfused *forbesi*	28	25	—	—	5	12	+70	+75	0·03	0·15	2·6	1·2	6·5	5
10-J-1	Perfused *forbesi*	—	35	—	—	—	15	—	+71	—	0·04	—	2·9	—	—
16-J-1	Perfused *forbesi*	30	30	—	—	—	—	+70	+76	0·05	0·10	2·4	1·5	—	—
16-J-2	Intact *forbesi*	60	60	33	40	—	—	+59	+51	0·10	0·10	3·5	2·9	7	—
22-J-1	Perfused *forbesi*	—	27	—	—	—	18	—	+90	—	0·15	—	1·8	—	—
23-J-1	Perfused *forbesi*	—	32	—	—	—	35‡	—	+78	—	0·06	—	3·0	—	—
24-J-1	Perfused *forbesi**	—	15	—	—	—	19	—	+95	—	0·05	—	1·4	—	6·5

* From living squid. † For 110 mM-Ca outside. ‡ For 110 mM-Ca outside as well as low ionic strength inside.

The shift of the $I-V$ curve was measured as the displacement of its peak towards a more positive potential in comparison with its standard position of -10 mV for an intact axon in 10 mM-Ca.

solution and bathed in Na- and K-free ASW containing 110 mM-Ca and 300 nM tetrodotoxin, while Fig. 4*B* illustrates a similar experiment with high ionic strength perfusion in a medium containing 10 mM-Ca and 1000 nM-tetrodotoxin. The membrane potential was held at respectively -70 and -100 mV, and voltage-clamp pulses of ± 120 mV were applied in each case. Graphical addition of the records for these pairs of equal positive and negative pulses revealed, as may be seen in the plots below, that in neither case were they quite symmetrical, but contained components corresponding to an extra outward current during depolarization and an extra current flowing inwards after the end of the pulses. The asymmetry during the pulses could be ascribed to the passage of an ionic leakage current which usually, as shown in Fig. 5 for the experiment of Fig. 4*A*, increased in size more steeply on depolarization, together with

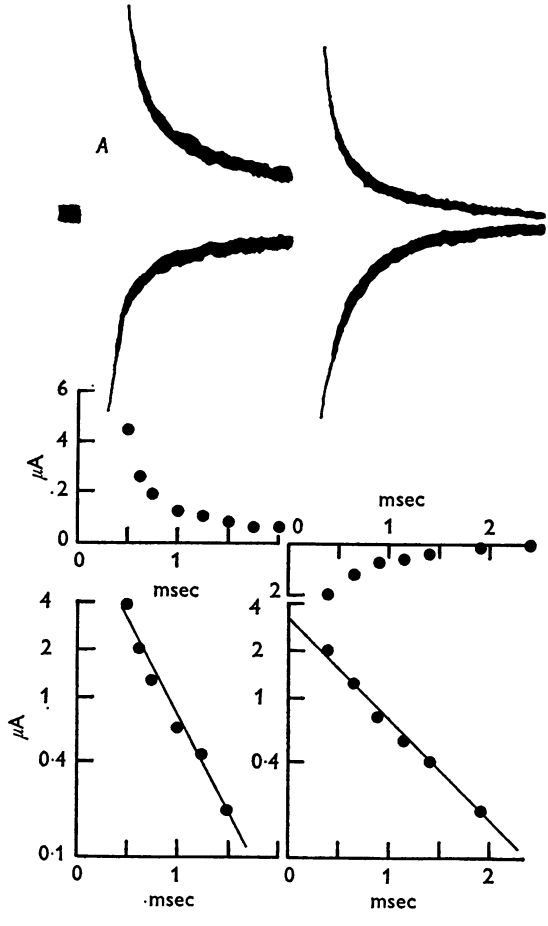

Fig. 4*A*. For legend see facing page.

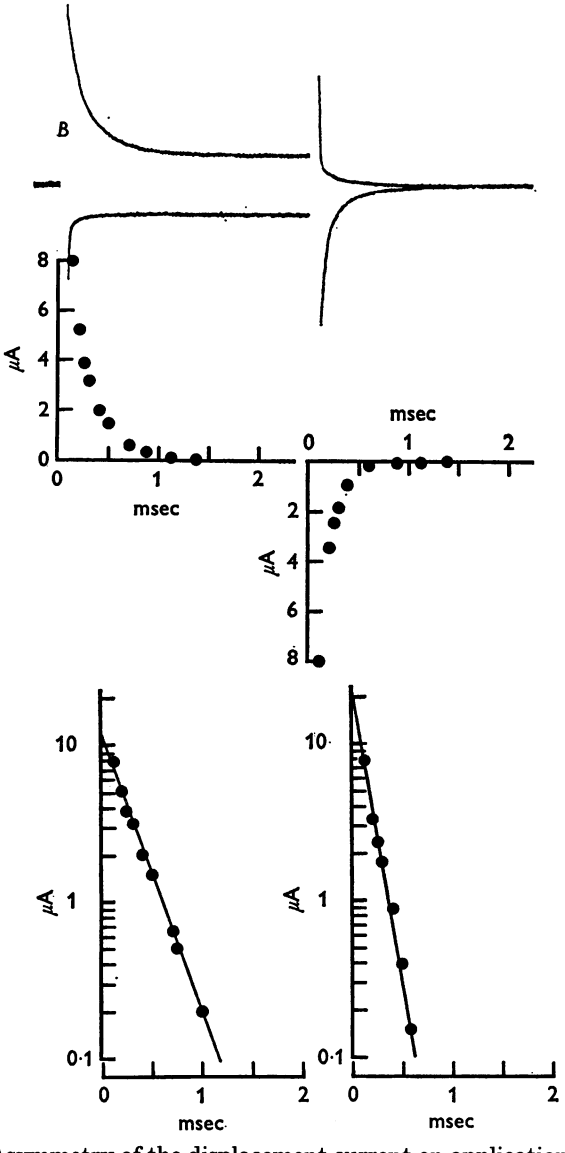

Fig. 4. Asymmetry of the displacement current on application of ± 120 mV voltage-clamp pulses. *A*. Axon perfused with 55 mM-CsF and bathed in Na- and K-free saline containing 110 mM-Ca and 300 nM tetrodotoxin; holding potential −70 mV; temperature 5° C; Expt. 23-J-1. *B*. Axon perfused with 300 mM-CsF + 600 mM sucrose and bathed in Na- and K-free saline containing 10 mM-Ca and 1000 nM tetrodotoxin; holding potential −100 mV; temperature 6° C; Expt. 23-N-2, from a later series. The result of graphical addition of the current records is plotted beneath each pair of tracings, both on the same scale linearly, and on a logarithmic scale. In *A*, the difference in sustained leakage current for the two pulses was 0·6 μA; this was subtracted before plotting logarithmically. In *B*, the leakage current did not rectify.

an outward current that rose abruptly at the start of the pulse and then declined exponentially with time. On restoration of the potential to the holding level there was another surge of current flowing in the opposite direction with a similar exponential time course. When the sustained ionic leakage current displayed a rectifying characteristic as in Figs. 4*A* and 5, the exponentially declining component of the difference current had a rectangular pedestal added to it during the pulse. On occasions when the leakage current did not rectify, as in Fig. 4*B*, this pedestal was absent. The asymmetry was much the same whether the tail of the capacity transient was fast, as in Fig. 4*B*, or was slowed down by lowering the internal ionic strength as in Fig. 4*A*.

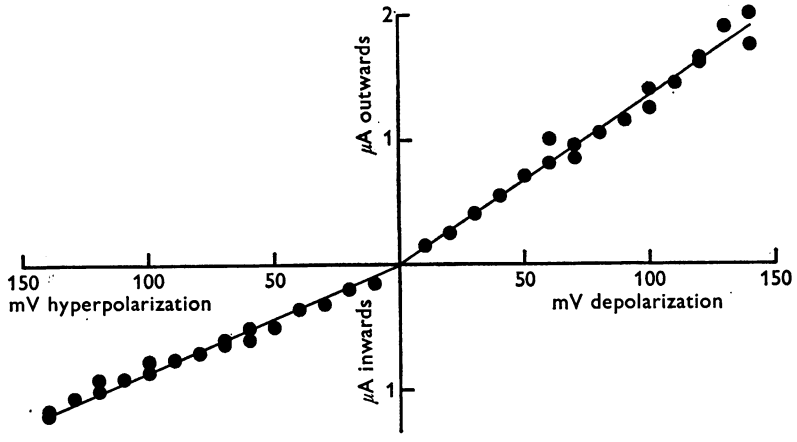

Fig. 5. Variation with potential of the steady current flowing at the end of 2 msec voltage-clamp pulses. Axon perfused with 55 mM-CsF and bathed in Na- and K-free saline containing 300 nm tetrodotoxin and 110 mM-Ca. Experiment 23-J-1. Temperature 5° C. Membrane area 0·071 cm². Slopes of lines correspond to membrane resistances of 5050 Ω cm² for depolarizing pulses and 8450 Ω cm² for hyperpolarizing pulses. Membrane potential plotted relative to a holding potential of −100 mV.

This method of investigating the asymmetries was somewhat laborious, and since the membrane current had to be recorded at a rather high gain, the difference plots were apt to be excessively noisy. Both these disadvantages could be overcome by using a signal averager to do the addition and at the same time to improve the signal–noise ratio by summing the differences in the current records for 60 pulses of each polarity. The remainder of this paper will be devoted to a discussion of the principal characteristics of the transient membrane currents flowing at the beginning and end of depolarizing voltage-clamp pulses, recorded with the help of a Princeton Waveform Eductor in axons in which the Na and K currents had been abolished.

Displacement of membrane charges during and after a step in membrane potential

Fig. 6 shows a family of records obtained in the course of an experiment using the signal averager. The external solution was Na- and K-free ASW containing 300 nM saxitoxin, and the axon was perfused internally with low ionic strength CsF solution. The results confirm the conclusions of the

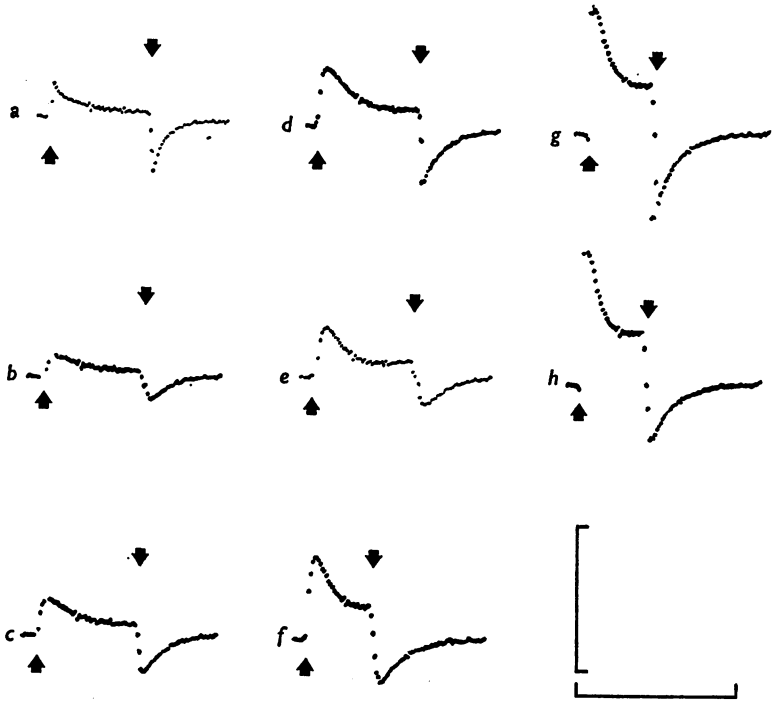

Fig. 6. Records of the asymmetrical displacement current obtained by adding together with the signal averager the membrane currents for 60 depolarizing and 60 hyperpolarizing pulses, starting and finishing at the arrows. Axon perfused with 55 mM-CsF. External solution was Na-, K- and Mg-free saline containing 300 nM saxitoxin. Pulse frequency 2 sec^{-1}, polarity changed every 5 sec. Duration of blanking pulses 50 μsec. Pulse amplitude, *a–h*, 40–110 mV. Resting membrane potential −52 mV, holding potential −70 mV. Vertical bar 5·56 μA; horizontal bar 2500 μsec. Temperature 6·3–7·0° C. Experiment 10-J-1.

preceding section in showing that the difference between the capacity transients for voltage-clamp pulses equal in size but opposite in sign has three components: (1) during the application of a depolarizing pulse there is an extra outward current which rises quickly to a peak and then decays

exponentially; (2) immediately following the end of the pulse there is a surge of membrane current in the opposite direction decaying to zero with a similar time course; (3) the first component is superimposed on an ionic leakage component denoted as ΔI_L which is usually rectangular, that is to say time-independent, but sometimes has a more complex time course.

After the steady outward current ΔI_L still flowing at the end of the pulse had been subtracted from the records, the time course of component (1) could be examined. When plotted semilogarithmically against time, the later points (beyond about 200 μsec after the start of the pulse) always lay nicely on a straight line like those in the lower sections of Fig. 4*A* and *B*, so that the current accurately followed an exponential with a single time constant τ_{on}. Component (2) similarly had a single time constant τ_{off}. The behaviour of the current during the first 200 μsec was somewhat variable. Thus in Fig. 6*a*, *g* and *h* it reached its peak within the interval of three memory addresses affected by the 50 μsec blanking pulse, but in *b*–*f* the peak apparently occurred with too long a lag after the start and finish of the pulse to be explained away by the blanking.

There are several possible explanations for the delay: (*a*) it could be due to the occurrence of an early asymmetry in the leakage current, for example a delayed rise on depolarization or an initial overshoot on hyperpolarization, producing in effect a current component in the opposite direction to the main one that decays with a time constant of around 60 μsec; (*b*) it could result from a recording artifact such as failure of the amplifier gain to recover instantaneously after the peak of the capacity transient, or on termination of the blanking pulse; (*c*) it could be a genuine feature of the time course of the displacement current; (*d*) the tacit assumption that there is no reverse displacement of mobile charges during the hyperpolarizing pulse may sometimes be incorrect. Tests made to explore the origin of the phenomenon gave disconcertingly variable results, but in later experiments it has become clear both that the leakage current may behave in a more complicated fashion than was at first supposed, in line with possibility (*a*), and that in some axons the mid-potential V' (see p. 419) of the steady-state distribution curve for the mobile charges may be somewhat more negative than Fig. 15 suggests. In such cases, unless the holding potential is very large, there is an appreciable backward transfer of charge on hyperpolarization, and in difference records of the type presented in Fig. 6, the peak of the displacement current is delayed in precisely the observed manner (see eqn. (15)). Armstrong (1974, fig. 10) has given the same explanation to account for the time course of his displacement current recordings. We conclude that (*d*) is probably the main cause of the delay in the peak, but (*a*), (*b*) and (*c*) may on occasion contribute to it. In the present series of experiments the first

200 μsec was routinely ignored when fitting exponentials to the records, which to some extent cuts out the error from reverse charge displacement.

The theoretical treatment given on p. 428 indicates that on changing the membrane potential the asymmetrical displacement current should display a time constant determined exclusively by the new potential level. Hence τ_{on} should vary systematically with pulse size but should be independent of the initial holding potential V_H, while τ_{off} should vary with V_H but not with pulse size. This expectation proved in general to be valid, as may be seen in Fig. 7, which illustrates the results of an experiment in which the time constants were first measured with different pulse sizes at

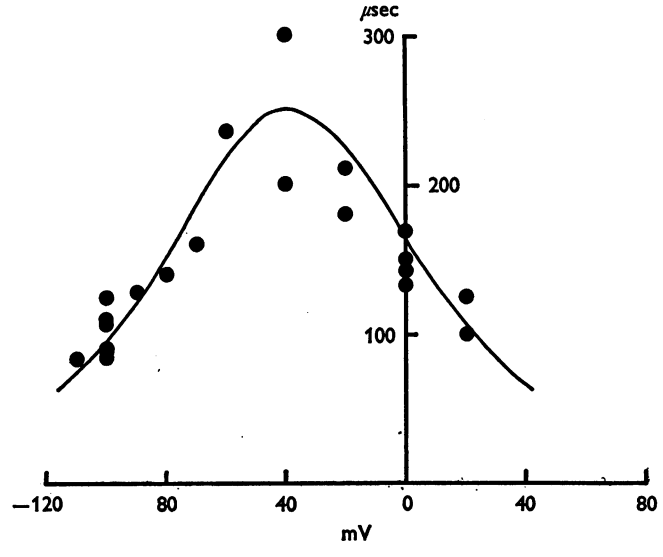

Fig. 7. The relationship between the time constant, τ, and absolute membrane potential. Experiment 5-J-2; intact axon in Na- and K-free tetrodotoxin saline with 10 mM-Ca; temperature 8·9° C. Either the holding potential was kept fixed at −100 mV while the pulse size was varied between 40 and 120 mV, or the holding potential was changed between −110 and −70 mV with a parallel variation in pulse size so that the potential during the pulse was always 0 mV. The curve is drawn according to eqn. (18) with $\tau_{max} = 250$ μsec, $V' = -40$ mV, and $kT/z'e = -19$ mV. In this and later Figures the abscissa shows absolute membrane potential, inside minus outside.

one holding potential, and then with pulses that always took the membrane potential to 0 mV but returned it to different values of V_H. The precise form of the relation between τ and potential will be considered later, and it need only be noted here that the maximum was usually reached in the neighbourhood of −30 mV, and that τ_{on} fell steadily as the potential was

TABLE 3. Variation in charge displacement and its time constant with membrane potential during the pulse

Expt. no.	Membrane area (cm^2)	Temp. (°C)	Holding potential V_H (mV)	Potential during pulse V_P (mV)	Extrapolated current at zero time: $I_{DO,on}$ (μA)	Extrapolated current at zero time: $I_{DO,off}$ (μA)	Time constant: τ_{on} (μsec)	Time constant: τ_{off} (μsec)	Charge displacement: Q_{on} (pC)	Charge displacement: Q_{off} (pC)	Leakage current ΔI_L (μA)
1-J-3	0·056	9·5	−80	−40	1·7	3·7	253	119	440	440	0·3
				−20	3·7	6·8	278	137	1030	930	0·8
				0	7·5	9·5	180	148	1350	1410	1·5
				+20	12·7	9·5	115	148	1460	1410	2·3
4-J-3*	0·043	7·5	−80	−20	1·7	3·4	314	114	520	380	0·4
				0	2·9	5·0	224	151	650	760	0·8
				+20	6·2	6·0	159	151	980	910	1·2
				+40	9·9	6·0	105	151	1030	910	1·5
5-J-1*	0·049	8·5	−100	−40	2·1	5·7	360	96	750	540	0·3
				−20	2·7	8·4	303	108	810	900	0·5
				−10	5·0	11·5	238	101	1190	1160	0·8
				+10	10·0	15·9	162	108	1620	1720	0·9
5-J-2*	0·045	10·5	−100	−60	1·3	3·8	216	85	290	320	0·1
				−50	2·0	5·8	250	87	490	510	0·3
				−40	2·0	6·7	281	95	560	640	0·3
				−20	4·2	8·2	242	102	1010	840	0·7
				0	7·8	14·2	190	106	1480	1500	1·3
				+20	12·5	14·4	116	108	1450	1550	1·8
9-J-1	0·061	7·5	−70	−20	0·8	5·6	360	87	280	480	0·3
				0	1·6	5·5	433	137	690	760	0·7
				+20	3·8	6·3	267	187	1000	1170	1·3
				+40	5·6	9·6	216	168	1210	1610	2·7
				+60	10·9	10·0	137	168	1490	1680	4·3
10-J-1	0·055	6·8	−70	−30	0·9	2·4	462	202	410	490	0·2
				−20	1·0	—	476	—	480	—	0·2
				−10	1·5	3·0	467	259	710	780	0·3
				0	2·8	3·5	374	288	1050	1010	0·4
				+10	3·0	—	274	—	820	—	0·6
				+20	3·6	3·5	242	274	870	960	1·0
				+30	5·6	4·2	190	274	1060	1150	1·4
				+40	6·7	4·1	173	275	1160	1130	1·7
				+50	8·3	4·0	149	273	1240	1090	2·2
24-J-1	0·055	6·0	−81	−30	0·4	0·7	400	188	160	130	0·05
				−20	0·6	1·4	476	198	290	280	0·05
				−10	0·8	1·1	512	288	410	320	0·07
				0	1·5	1·3	426	288	640	370	0·07
				+10	2·4	1·4	252	280	600	390	0·07
				+20	2·6	—	252	—	660	—	—
				+30	5·4	—	216	—	1160	—	—
				+40	5·6	—	180	—	1010	—	—

* Intact axon.

driven to increasingly positive levels. One respect in which the behaviour of the system did not conform with that predicted for the simplest type of model was that there was a tendency for τ_{off} to be nearly twice as great for the largest pulses as it was for the smallest ones (see Tables 3 and 6); and when the duration of a pulse of constant amplitude was varied, τ_{off} steadily increased with pulse length. This dependence of τ_{off} on the previous history of the membrane potential was not investigated in any detail in the present series of experiments, but is an important point for further exploration in the future.

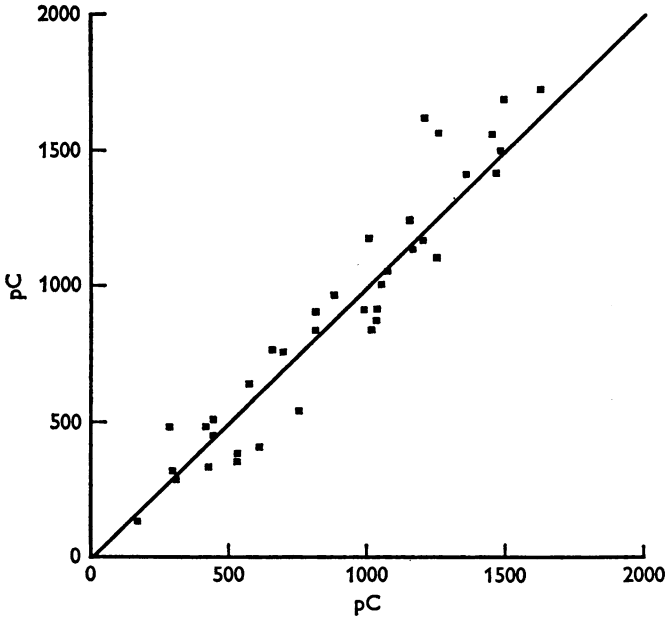

Fig. 8. The balance of charge displacement at the beginning and end of the pulses. Data from Table 3, plotting Q_{on} against Q_{off}. The least-squares regression line had a slope of $0{\cdot}976 \pm 0{\cdot}050$ (S.E.).

If the exponentially changing components of the asymmetrical membrane current are to be identified with the displacement of charged particles that are an integral part of the membrane, then the total transfer of charge in one direction at the beginning of the pulse should be exactly balanced by the transfer in the other direction at the end. In order to test this equality, experiments were chosen in which the pulses were long enough for the steady leakage current ΔI_L to be estimated reliably, and after subtracting it, exponentials were fitted to the points from 200 μsec onwards. The sizes of the time constants and of the extrapolated value of the displacement current at zero time, I_{DO}, were determined. The

total charge transfer during the pulse was calculated from the integral $Q_{on} = I_{DO.on} \cdot \tau_{on}$, and that at the end of the pulse from $Q_{off} = I_{DO.off} \cdot \tau_{off}$, Q_{on} and Q_{off} were then plotted against one another as shown in Fig. 8, and the slope of the line fitted by the method of least squares was found not to be significantly different from unity. One source of uncertainty in thus comparing Q_{on} and Q_{off} was the rather large correction to $I_{D,on}$ that sometimes had to be made for ΔI_L. However, later experiments in which ΔI_L was greatly reduced by bathing the axon in a Cl-free solution, and in which the asymmetry in the charge displacement was measured directly from single sweep records without recourse to the signal averager, confirmed the equality of Q_{on} and Q_{off}. It could also be objected that the

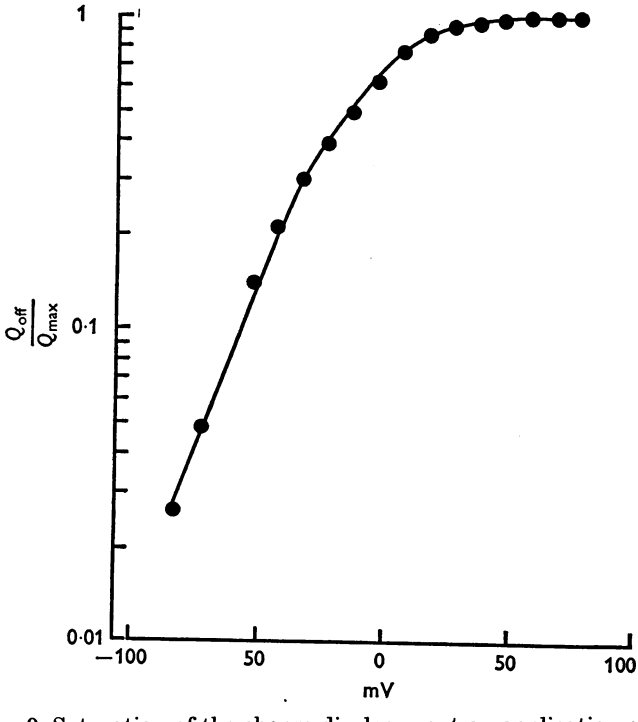

Fig. 9. Saturation of the charge displacement on application of sufficiently large voltage-clamp pulses. Ordinate: Q_{off}/Q_{max}, logarithmic scale. Abscissa: membrane potential during the depolarizing pulse. The records for the restoration of the charge at the end of the pulse were indistinguishable for 140, 160 and 180 mV pulses, and their area corresponded to a displacement of 2440 $e/\mu m^2$. Axon perfused with 50 mM-CsF and bathed in Na- and K-free isethionate saline containing 300 nM tetrodotoxin. Holding potential − 103 mV. Temperature 6° C. The same data replotted as in Fig. 15 gave a slope of 18 mV for an e-fold change. From a later series of experiments conducted with the help of Dr B. Rudy, whose results are not included in Tables 3 and 5.

charge transfer calculated by extrapolation to zero time was sometimes as much as 30% greater than that obtained from the total area of the records; but this generally applied both to Q_{on} and to Q_{off}, and so had a lesser effect on the balance between them. In any case, measurement of the charge transfer by planimetry in these experiments still revealed no systematic difference between Q_{on} and Q_{off}.

Another criterion that has to be satisfied is that the charge displacement should reach a definite limit when large enough pulses are applied to the membrane. In the present series of experiments we did not make many observations with pulses greater than 120 mV, and although, as may be seen in Table 5, Q_V was generally raised to within 5% of the saturation level, the existence of a final plateau was not satisfactorily established. This point was taken up again later, and Fig. 9 shows the result of applying pulses up to 180 mV in amplitude to the membrane. The values of Q_{off} only are plotted here, because when such large pulses were employed the leakage current ΔI_L was embarrassingly large compared with the displacement current, and tended to lose its time-independence. Although Q_{on} then became difficult to measure with certainty, there was no good reason to doubt that it did not remain equal to Q_{off}. This and several similar experiments therefore furnished an adequate demonstration that above about 140 mV there was no further asymmetrical transfer of charge, so that saturation of the system of mobile charges with which we are concerned had indeed been achieved.

The displacement of membrane charges in intact axons

Cole & Moore (1960) demonstrated that at 20° C hyperpolarization of the membrane to -110 mV before applying a voltage-clamp pulse delays the activation of the K system by some 300 μsec. As we have verified in unpublished experiments, the delay is even greater when the external calcium concentration is raised (Frankenhaeuser & Hodgkin, 1957). This effect can usefully be exploited to measure the displacement currents in intact axons without prior perfusion to block the potassium channels, by recording $I_{D,on}$ during the interval before any appreciable potassium current starts to pass across the membrane. The employment of intact axons has several advantages in addition to being an easier technique. Thus the peak Na conductance is generally greater (see Table 2) and the survival time of the axon is prolonged. Moreover, undesirable effects of intracellular perfusion like the partial abolition of Na inactivation described by Chandler & Meves (1970*b*) are avoided, together with the shifts of the curves relating the voltage-dependent parameters to membrane potential brought about by a reduction in internal ionic strength (Chandler, Hodgkin & Meves, 1965). Apart from differences related to these shifts

(see p. 419), the results obtained from intact axons were very similar to those for perfused axons, as may be judged from Table 3. This disposes of the possibility that the displacement current is merely an artifact resulting from replacement of the axoplasm with unphysiological solutions.

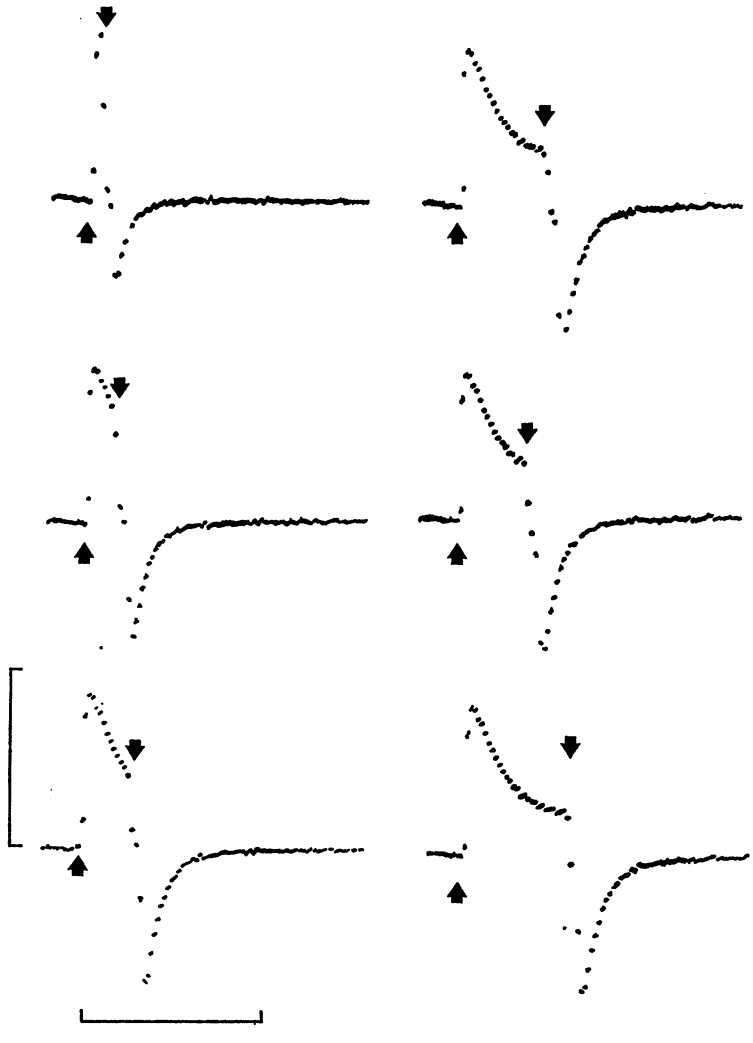

Fig. 10. Variation in charge displacement with pulse duration. Intact axon from *L. vulgaris* in Na- and K-free saline with 300 nM tetrodotoxin. Resting membrane potential − 55 mV; holding potential − 100 mV. Pulse amplitude 110 mV throughout, pulse duration 100–600 μsec, 50 μsec blanking. Axon diameter 625 μm. Temperature 8·5° C. Vertical calibration bar 8·35 μA. Horizontal bar 1000 μsec.

Having established that there is an exact balance between the displacement of charge at the start of the pulse and at its termination, we can determine τ_{on} from measurements of the integrated transfer of charge on repolarization, Q_{off}, after pulses of varying duration, without having to estimate ΔI_L. Figs. 10 and 11 illustrate the results of an experiment of this

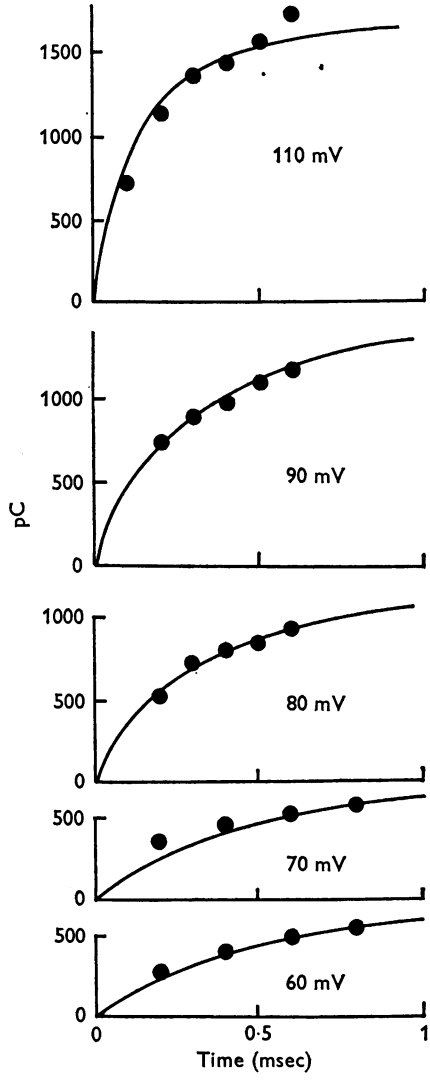

Fig. 11. Charge displacement plotted as a function of pulse duration for the pulse size shown against each curve. Q_{off} was calculated for each duration in sets of records like that shown in Fig. 10. For other experimental details see legend to Fig. 10.

kind on an intact axon. For each pulse amplitude, several records were made with pulse durations increasing in steps from 100 to 800 μsec, a typical set being shown in Fig. 10, Q_{off} was calculated as before for each record, and the values were plotted against pulse length as in Fig. 11. The time constants of the exponentials that gave the best fit for each set of values agreed well with measurements of τ_{on} for the longest pulse in each group of records.

Measurement of displacement current before treatment with tetrodotoxin

It could be objected that the displacement current measured in this fashion was an artifact arising in some way from the blocking of the Na channels with tetrodotoxin or saxitoxin. This proposition was examined by measuring the asymmetrical membrane currents in an axon perfused with low ionic strength CsF solution before and after treatment with saxitoxin. In order to obtain the records in Fig. 12, 90 mV pulses of varying duration were applied to an axon perfused internally with low ionic strength CsF solution and bathed externally in Na- and K-free ASW. 300 nM saxitoxin was then added to the external solution, and 10 min later the displacement current records shown in Fig. 13 were made, with the pulse duration now kept constant at 800 μsec and the pulse size varied between 50 and 130 mV. It is seen that in both sets of records there was the usual surge of inward current on repolarization, the two traces for pulses of the same size and duration, *d* in Fig. 12 and *c* in Fig. 13, having τ_{off}'s of 156 and 136 μsec respectively, and amplitudes differing by not more than 20%. Until the Na channels had been blocked, however, there was clearly an additional source of outward current during the pulse, whose approximate time course is indicated in Fig. 12(*e*). This and its size (see Chandler & Meves, 1965) are consistent with the idea that it arose from an outward passage of caesium ions through the Na channels. It inevitably obscured the displacement current flowing at the same time, but analysis of the size of the inward 'tails' of current seen in Fig. 12 when the pulse duration was changed, using the procedure discussed on p. 414, yielded an estimate for τ_{on} of 320 μsec, which compares reasonably well with the figure of 290 μsec observed for a pulse of the same size after applying saxitoxin (Fig. 13*c*). Hence the only obvious effect of the saxitoxin was to abolish the outward caesium current, and there is no reason to suppose that the displacement currents were affected in any way.

Effect of temperature

If the exponentially declining components of the asymmetrical membrane current do indeed arise from the displacement of charged particles

that are an integral part of the membrane, a change in temperature would be expected to alter the time constants τ_{on} and τ_{off}, but not the total transfer of charge Q_{on} and Q_{off}, since there is no obvious reason why the total number of particles should be temperature-dependent. In order to test this point, systematic observations of the effect of temperature were made on five axons, and the results were more or less in accordance with

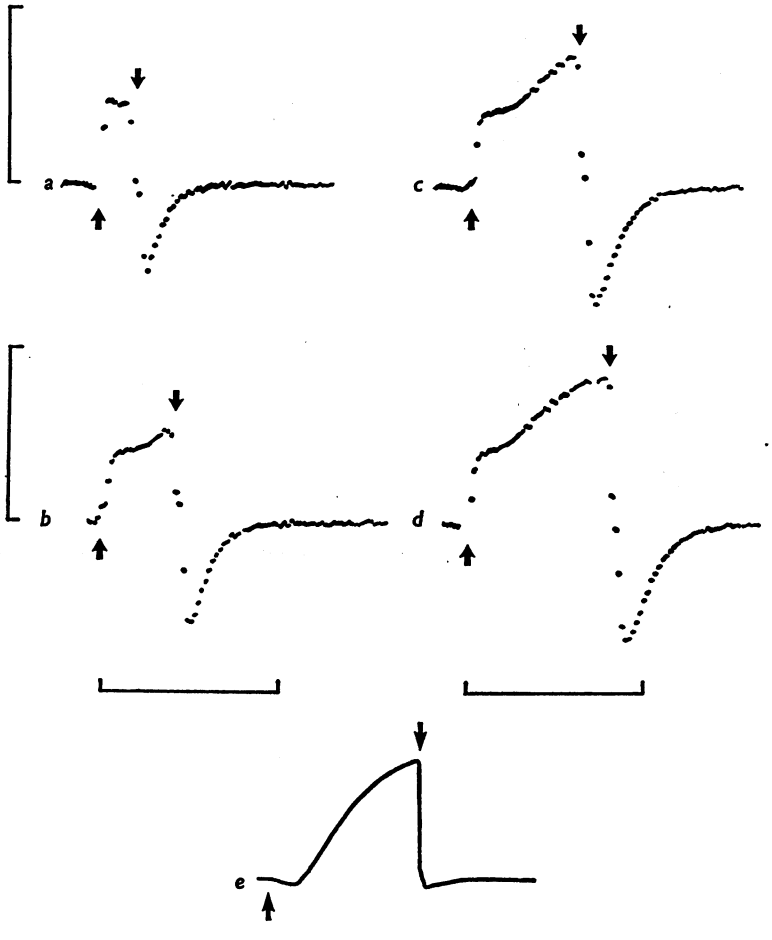

Fig. 12. Asymmetrical displacement currents recorded in Na- and K-free saline before treatment with saxitoxin to block the Na channels. Axon perfused with 55 mM-CsF. Resting membrane potential −58 mV. Holding potential −90 mV. Pulse size 90 mV throughout, duration 200–800 μsec, 50 μsec blanking. Temperature 8·5° C. Vertical calibration bars 140 μA/cm². Horizontal bars 1000 μsec. Experiment 9-J-1. *e* indicates the approximate time course of the difference between record *d* in this Figure and *c* in Fig. 13.

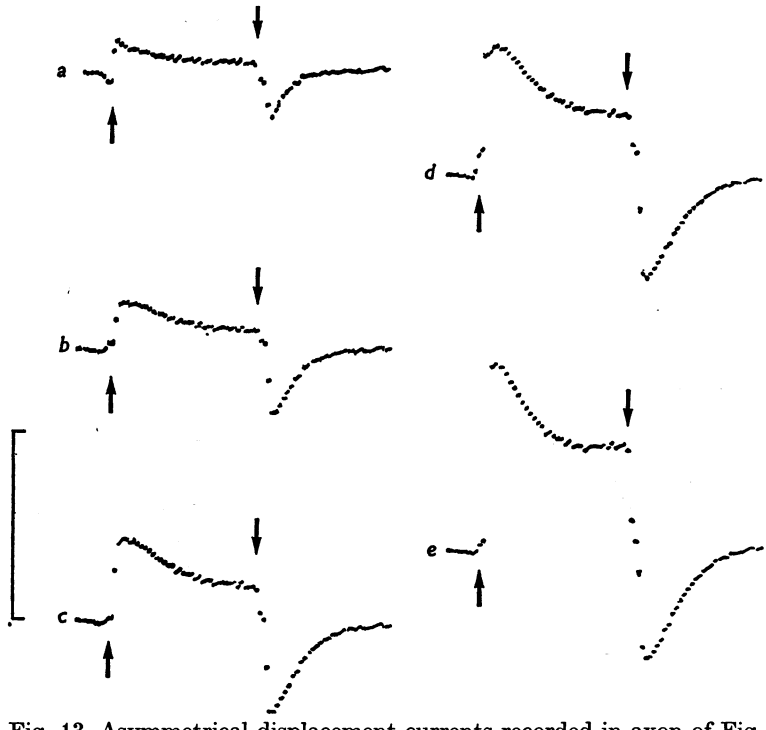

Fig. 13. Asymmetrical displacement currents recorded in axon of Fig. 12, 10 min after adding 300 nM saxitoxin to the external medium. For this set of records the pulse duration was kept fixed at 800 μsec, and its size was varied between 50 mV in *a* and 130 mV in *e*. Temperature 7·3° C. Vertical calibration bar 140 μA/cm^2.

expectation. The records reproduced in Fig. 14 illustrate clearly the marked increase in the time constants when the temperature was lowered, and the results summarized in Table 4 show that the Q_{10} for τ_{off} ranged from 1·7 to 3·2, with an average value of $2{\cdot}5 \pm 0{\cdot}3$. It turned out that ΔI_L increased appreciably on warming, making the values of τ_{on} and Q_{on} hard to measure reliably at the higher temperature. Table 4 therefore contains only data for the displacement current during repolarization. Within the accuracy of the measurements, Q_{off} did not change significantly with temperature.

Dependence on potential of total charge displaced

An example of the saturation of charge displacement at increasingly positive membrane potentials has already been given in Fig. 9. The steepness and position of the lower part of the curve relating the total charge displaced to absolute membrane potential were characteristics of the system that it was important to investigate, and measurements of the

dependence of Q_{on} and Q_{off} on pulse size were made for most of the axons, giving the results listed in Table 5. The charge displacement Q_V for depolarization to a potential V was calculated, generally as $\frac{1}{2}(Q_{on}+Q_{off})$, and

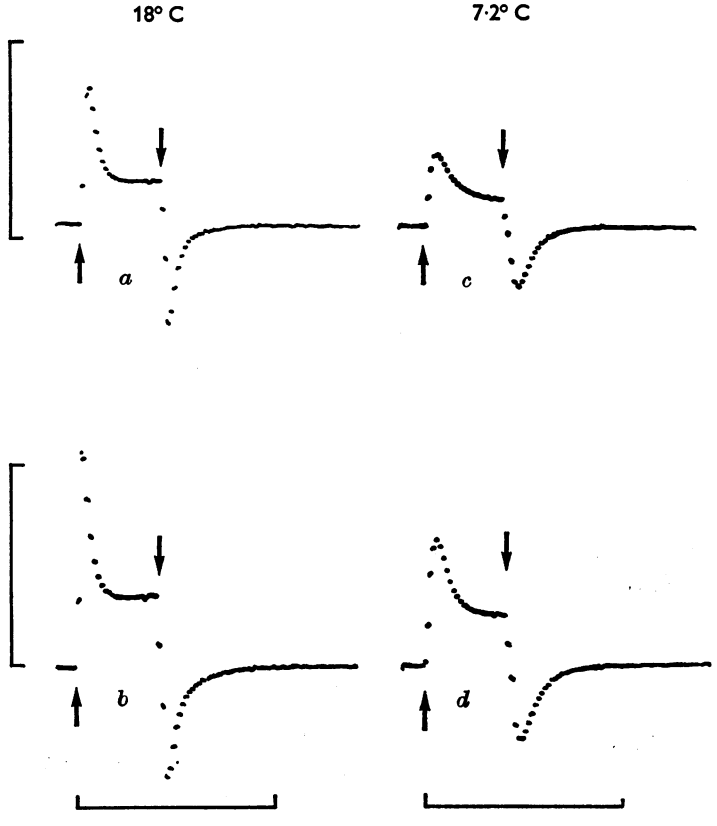

Fig. 14. The effect of temperature on charge displacement. Axon perfused with 55 mM-CsF. Holding potential −90 mV, pulse size 90 mV for *a* and *c*, 120 mV for *b* and *d*. Pulse duration 1000 μsec throughout. Left hand records made at 18° C, right hand at 7·2° C. From recordings with faster sweeps, τ_{off} was estimated as 108 or 109 μsec at 18° C, and 180 or 190 μsec at 7·2° C. Experiment 9-J-1. Vertical calibration bars 4·2 μA, horizontal bars 2500 μsec.

normalized by dividing it by its value at saturation, Q_{max}. The quantity $\frac{Q_V/Q_{max}}{1-Q_V/Q_{max}}$ was then plotted on a logarithmic scale against potential. As explained on p. 427 the slope of the straight line thus obtained yields an estimate for the effective valency of the charged particles, that is to say for their actual charge multiplied by the fraction of the electric field that acts upon them. The potential at which the ratio equals unity is the

TABLE 4. Effect of temperature on time constant and charge displacement at end of pulse

Expt. no.	Potential during pulse (mV)	Temperature (°C)	Time constant τ_{off} (μsec)	Current at $t = 0$ I_{DO} (μA)	Charge displaced $\tau_{off} \cdot I_{DO}$ (pC)	Q_{10} for Time constant	Q_{10} for Charge displaced
1-J-2	+20	9	137	12·3	1680	−3·2	−1·05
		19	43	41·8	1800		
		9	137	15·4	2110		
1-J-3	0	8·5	152	12·2	1850	−2·1	+1·03
		20	65	29·2	1900		
		9	152	12·0	1820		
4-J-3	0	7·5	151	6·2	940	−2·3	+1·13
		20	54	20·0	1080		
		8	151	6·0	910		
9-J-1	0	7·2	190	12·0	2280	−1·7	+1·09
		18	109	23·0	2510		
24-J-1	−10	6·0	288	0·66	190	−3·1	−1·01
		7·5	274	0·68	186		
		9·3	230	0·71	163		
		11·8	144	1·13	163		
		12·3	144	1·17	168		
		13·7	135	1·46	197		
		16·7	110	1·55	170		

transition potential at which the mobile charges are equally distributed in the two energy states.

As may be seen in Fig. 15 and Table 5, the slope of the plots was roughly the same for all the axons, its average value being 19·4 mV for an e-fold change, which corresponds to an effective valency of −1·3. The negative sign here is simply a consequence of the definitions adopted in writing eqn. (3); we have, of course, no way of distinguishing between negative charges moving inwards on depolarization of the membrane, and positive

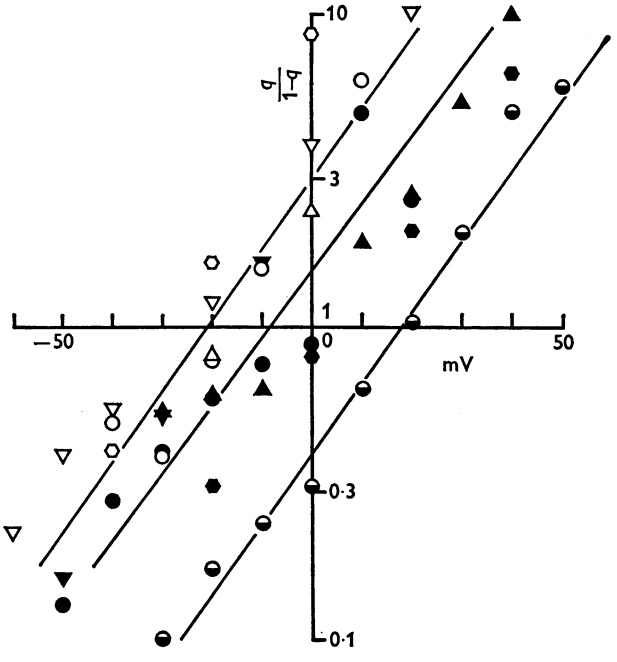

Fig. 15. The steepness of the steady-state relationship between charge displacement and membrane potential. Ordinate: $q/(1-q)$ where q is Q_V/Q_{max}, values from Table 5, logarithmic scale. Abscissa: membrane potential during the depolarizing voltage-clamp pulse. The lines are drawn by eye to fit the averages of $kT/z'e$ and V' from Table 5 for the individual experiments grouped thus: (1) 1-J-3 (◇), 4-J-3 (△), 5-J-1 (○) and 5-J-2 (▽); (2) 9-J-1 (◆), 10-J-1 (▲), 22-J-1 (▼) and 24-J-1 (●); (3) 23-J-1 (◒).

charges moving outwards. The plots did not, however, all occupy the same position laterally. For three intact axons and one perfused with high, ionic strength (275 mM) CsF, the mean transition potential V' was $-21{\cdot}5 \pm 3{\cdot}5$ mV, while for four others perfused with low ionic strength (55 mM) CsF it was $-8{\cdot}0 \pm 4{\cdot}9$ mV. A single axon also perfused with low ionic strength CsF but with 110 mM-Ca^{2+} in the external medium instead of

TABLE 5. Steady-state displacement of charge as a function of membrane potential

Expt. no.	Condition of axon	Holding potential V_H (mV)	Potential during pulse V_P (mV)	Charge displaced Q_V ($e/\mu m^2$)	Saturation value of Q_V Q_{max} ($e/\mu m^2$)	$\frac{Q_V}{Q_{max}}$	Slope $kT/z'e$ (mV)	Transition potential V' (mV)
1-J-3	Perfused 275 mM-CsF	−80	−40	490	1720	0·29	14	−27
			−20	1060		0·62		
			0	1540		0·90		
			+20	1600		0·93		
4-J-3	Intact	−80	−20	660	1470	0·45	19	−16
			0	1030		0·70		
			+20	1370		0·93		
			+40	1410		0·96		
5-J-1	Intact	−100	−40	820	2480	0·33	22	−15
			−30	680		0·27		
			−20	1090		0·44		
			−10	1500		0·61		
			+10	2130		0·86		
5-J-2	Intact	−100	−60	420	2350	0·22	20	−28
			−50	660		0·28		
			−40	830		0·35		
			−20	1280		0·55		
			0	1860		0·79		
			+20	2140		0·91		
9-J-1	Perfused 55 mM-CsF	−90	−20	390	1660	0·24	20	+4
			0	740		0·45		
			+20	1110		0·67		
			+40	1440		0·87		
			+60	1620		0·98		
10-J-1	Perfused 55 mM-CsF	−70	−30	510	1430	0·36	26	−7
			−20	540		0·38		
			−10	550		0·39		
			+10	930		0·65		
			+20	1040		0·73		
			+30	1200		0·84		
			+40	1300		0·91		
			+50	1340		0·94		

TABLE 5 (*cont.*)

Expt. no.	Condition of axon	Holding potential V_H (mV)	Potential during pulse V_P (mV)	Charge displaced Q_V ($e/\mu m^2$)	Saturation value of Q_V Q_{max} ($e/\mu m^2$)	$\frac{Q_V}{Q_{max}}$	Slope $kT/z'e$ (mV)	Transition potential V' (mV)
22-J-1	Perfused 55 mM-CsF	−70	−50	260	1870	0·14	17	−20
			−30	650		0·35	(17)	(−13)
			−10	1150		0·62	(21)	(−26)
			+10	1750		0·94		
			+30	1780		0·95		
			+50	1830		0·98		
23-J-1	Perfused 55 mM-CsF and high external [Ca]	−70	−40	100	2360	0·04	18	+19
			−30	220		0·09		
			−20	350		0·15		
			−10	460		0·20		
			0	560		0·24		
			+10	920		0·39		
			+20	1210		0·51		
			+30	1580		0·67		
			+40	1960		0·83		
			+50	2010		0·85		
			+60	2270		0·96		
			+70	2270		0·96		
24-J-1	Perfused 55 mM-CsF	−80	−50	190	1600	0·12	19	−9
			−40	350		0·22		
			−30	490		0·31		
			−20	600		0·38		
			−10	690		0·43		
			0	750		0·47		
			+10	1330		0·83		
			+20	1150		0·72		

In Expt. 23-J-1 the external solution contained 110 mM-Ca; in all the others only 10 mM-Ca. The value of Q_{max} was determined from a preliminary inspection of the data, and readjusted if necessary to obtain a good fit. The figures in brackets in the last two columns are results from other runs on the same axon.

10 mM had a transition potential of +19 mV. Although the variability of V' from one axon to the next was too great for hard and fast conclusions to be drawn about the size of these lateral shifts of the plots along the voltage axis, they were satisfactorily consistent with the observations of Chandler *et al.* (1965) on the effect of a reduction in internal ionic strength, and of Frankenhaeuser & Hodgkin (1957) on the effect of external Ca.

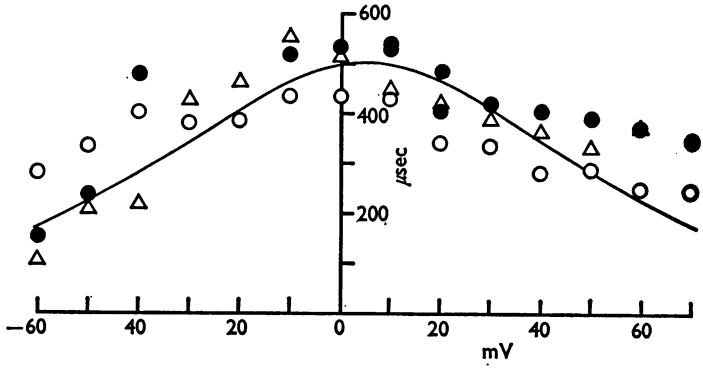

Fig. 16. The effect of external Ca concentration on τ_{on}. Ordinate: time constant at beginning of pulse. Abscissa: membrane potential during the pulse. ○, first run, in 110 mM-Ca. △, second run, in 10 mM-Ca. ●, third run, in 110 mM-Ca again. Axon perfused with 55 mM-CsF. Temperature 5° C. Holding potential −70 mV. Experiment 23-J-1. The curve is drawn according to eqn. (18) with τ_{max} = 500 μsec, V' = +5 mV, and $kT/z'e$ = −18 mV.

The action of Ca was further examined in an experiment in which sets of displacement current records were made for an axon exposed to 110, 10 and again 110 mM-Ca. As may be seen in Fig. 16, the time constant reached its maximum at a membrane potential between +5 and +10 mV in 110 mM-Ca, whereas in 10 mM-Ca the peak fell at about −10 mV. Its absolute magnitude was, however, unaffected by the change in Ca concentration. This reversible shift of the curve relating τ_{on} to potential in a positive direction on raising the external Ca again fits well with the effect of Ca on the $g_{Na} - V$ relation in *Loligo* axons (Frankenhaeuser & Hodgkin 1957; R. D. Keynes & E. Rojas, unpublished observations).

In other experiments, records were made with the external pH varied between 5 and 8. Neither τ_{on} nor Q_V was significantly altered, suggesting that over this pH range the degree of ionization of the charged particles under observation is constant.

Effect of local anaesthetics

It has been shown by Taylor (1959) that local anaesthetics like procaine act on the squid giant axon by depressing the Na conductance. It was

therefore of interest to examine their action on the displacement current. A 0·1 % solution of procaine in ASW at pH 8, which should have reduced g_{Na} by about half (Taylor, 1959), was first tried, but did not seem to have any marked effect on the displacement current, although subsequent analysis of the records showed a slight reduction. The concentration of procaine was therefore raised to 1 %, at which level the Na conductance in an intact axon was cut down to one-tenth of its unanaesthetized value, with excellent recovery afterwards (Fig. 17). The displacement current

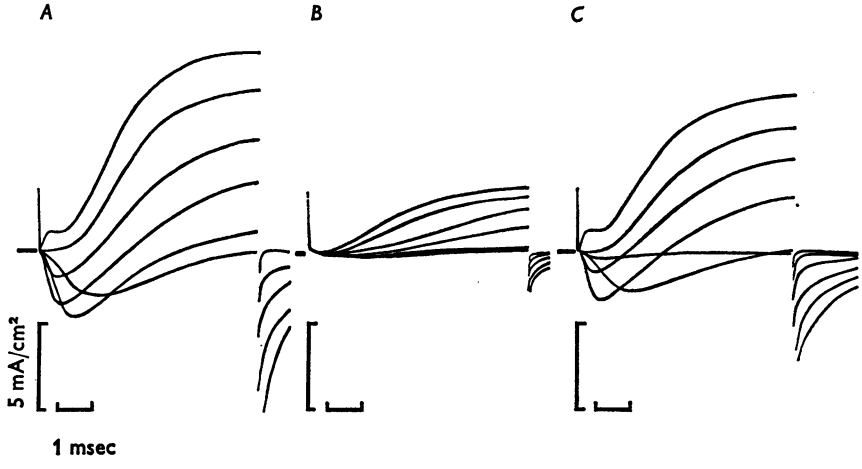

Fig. 17. Effect of 1 % procaine on Na and K currents. *A*. Membrane currents recorded in K-free ASW before treatment with procaine. Intact axon. pH of the external solution adjusted to 8 with Tris-Cl. Temperature 5·5° C. Voltage-clamp pulses of 40, 60, 80, 100, 120 and 140 mV. *B*. Membrane currents recorded in K-free ASW 15 min after adding 1 % procaine. External pH kept at 8. Voltage-clamp pulses as in *A*. *C*. Membrane currents recorded 25 min after removing the procaine. Voltage-clamp pulses as in *A*. Vertical calibration bars 5 mA/cm². Horizontal bars 1 msec. Experiment 16-J-2.

records shown in Fig. 18 were made during the same experiment, and exhibit a clear reduction in Q_V when 1 % procaine was present, with recovery which would presumably have gone to completion had more time been allowed. From the results for this and a similar experiment given in Table 6, it may be seen that Q_V was on average reduced to just under 40 % of its control value. In the experiment of Figs. 17 and 18 both τ_{on} and τ_{off} fell appreciably when the axon was treated with procaine, and declined still further during the recovery period. There was also some indication of a Ca-like shift in the curve relating τ_{on} to potential. These effects on the time constant seem consistent with the view (Seeman, 1972) that anaesthetics increase the fluidity of the lipid matrix of the membrane,

and indicate that the lipid must normally exercise some constraint on the ease with which conformational changes can take place in the protein molecules that constitute the Na channels. We cannot yet say exactly why the procaine decreases the amplitude of movement of the mobile charges, but these preliminary observations suggest that a more detailed investigation of the mechanism of interaction between local anaesthetics and the gating particles should prove rather profitable.

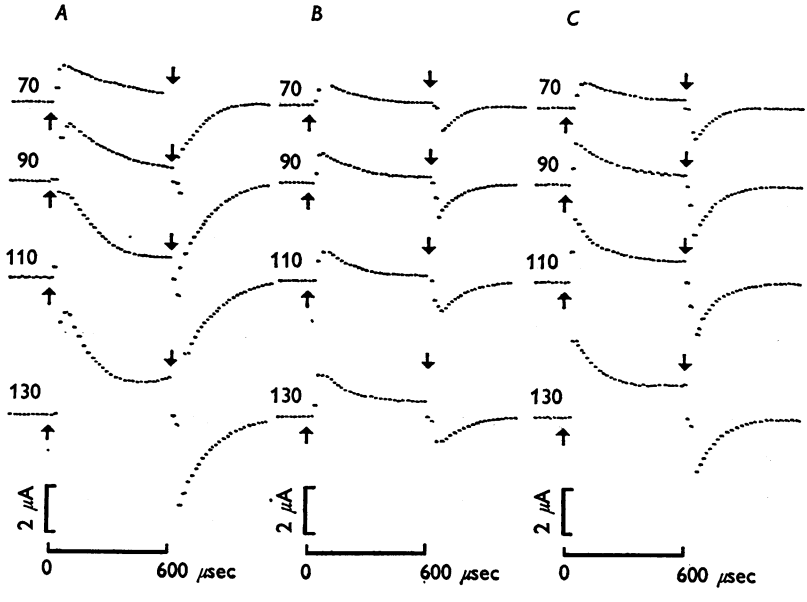

Fig. 18. Effect of 1 % procaine on charge displacement in axon of Fig. 17. The external solution was Na- and K-free ASW containing 300 nM tetrodotoxin at pH 8 throughout. *A*. Initial control. *B*. 10 min after application of 1 % procaine. *C*. 10 min after removing procaine. Holding potential −90 mV for all runs; size of voltage-clamp pulses in mV shown against each record. Temperature 5·3–5·5° C. Vertical calibration bars 2 μA; horizontal bars 600 μsec. Note that since the axon was intact and not perfused with CsF, outward K current became apparent towards the end of the 130 mV pulses. Experiment 16-J-2.

DISCUSSION

An essential criterion for regarding the sharply rising and exponentially declining components of the asymmetrical membrane current as due to the displacement of mobile charged particles or dipoles that form an integral part of the membrane is that the total transfer of charge in one direction at the start of the pulse should exactly balance that in the opposite direction at the finish. This point has been sufficiently well established

TABLE 6. The effect of 1 % procaine on charge displacement

Expt. no.	Potential during pulse (mV)	τ_{on} Control	τ_{on} Procaine (μsec)	τ_{on} After	τ_{off} Control	τ_{off} Procaine (μsec)	τ_{off} After	Q_{off} Control	Q_{off} Procaine (pC)	Q_{off} After
16-J-1	−10	552	348	—	205	103	—	1030	520	—
	+10	414	243	—	303	120	—	1910	770	—
	+30	339	266	—	264	120	—	1870	1090	—
	+50	243	218	—	324	150	—	2430	1520	—
	+70	217	217	—	313	142	—	2280	1660	—
16-J-2	−20	438	242	152	103	78	79	520	180	200
	0	317	278	180	124	115	111	720	180	300
	+20	132	134	158	154	126	104	820	280	400
	+40	125	118	105	160	128	113	800	230	430

Axon 16-J-1 was perfused with 55 mM-CsF; 16-J-2 was intact. Q_{on} was reduced on average to 39 % of the control value in 16-J-1 and to 37 % in 16-J-2; for Q_{off} the mean figures were respectively 57 and 31 %. In 16-J-2 the sodium conductance in procaine was 12 % of the control value, and after 1 hr in a procaine-free solution recovery was complete; only 20 min was allowed for recovery before remeasuring Q_{off}.

in Fig. 8 not to require further discussion. Before proceeding further with an analysis of the other features of our results, it is necesssary to consider some of the properties to be expected in a simple system of N identical and independent charged particles which are free to undergo a first-order transition between two states whose energy levels are determined by the electric field across the membrane. Suppose that in a steady state the average number of particles at or close to the inside of the membrane is N_1, and the average number at the outside is N_2. Application of Boltzmann's principle leads immediately to

$$\frac{N_1}{N_2} = \exp\left[\frac{-z'e}{kT}(V-V')\right], \tag{3}$$

where z' is the effective valency of each particle, i.e. the number of positive electronic charges that it carries multiplied by the fraction of the total field across the membrane that acts upon it; e is the absolute value of the charge on an electron; k is Boltzmann's constant; T is absolute temperature; V is the membrane potential, inside minus outside; V' is the potential at which $N_1 = N_2$. If then p is the fraction of the total particles on the inside, and $1-p$ the fraction on the outside,

$$p = \frac{N_1}{N_1+N_2} \quad \text{and} \quad 1-p = \frac{N_2}{N_1+N_2},$$

whence

$$\frac{p}{1-p} = \exp\left[\frac{-z'e}{kT}(V-V')\right], \tag{4}$$

or

$$p = \frac{\exp\left[\frac{-z'e}{kT}(V-V')\right]}{1+\exp\left[\frac{-z'e}{kT}(V-V')\right]}. \tag{5}$$

If at the holding potential V_H, $p = p_0$; and if on depolarization to potential V the total charge displacement is Q_V, whose saturation value is Q_∞, then writing

$$Q_{max} = z'e(N_1+N_2), \tag{6}$$

we have

$$Q_V = Q_{max}(p-p_0) \tag{7}$$

and

$$Q_\infty = Q_{max}(1-p_0). \tag{8}$$

Putting $q = Q_V/Q_\infty$ it follows that

$$\frac{q}{1-q} = \frac{p}{1-p} - \frac{p_0}{1-p}. \tag{9}$$

Hence if V_H is sufficiently large and negative for p_0 to be negligibly small, $q/(1-q)$ can be equated with $p/(1-p)$, and from eqn. (4) a semi-logarithmic

plot of $q/(1-q)$ against potential should give a straight line whose slope is $-z'e/kT$ and which crosses the axis at $V = V'$. In cases where $V_H - V'$ was less than -45 mV, p_0 was 0·1 or more, and eqn. (9) had to be applied to obtain corrected values for $p/(1-p)$. As has been seen in Fig. 15, the results gave plausible values for V' and the slope when plotted in this fashion, but

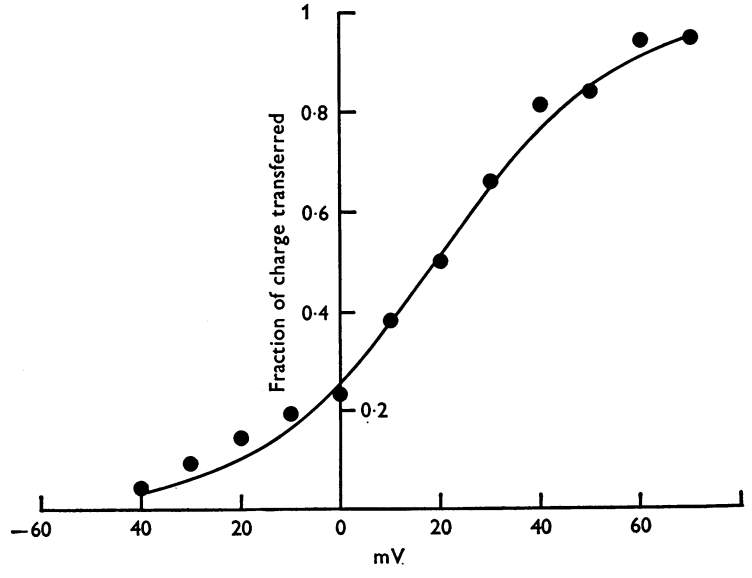

Fig. 19. The fraction of total charge transferred, Q_V/Q_{max}, plotted linearly as a function of membrane potential V_p. Experiment 23-J-1; axon perfused with low ionic strength CsF solution, in Na- and K-free tetrodotoxin saline with 110 mM-Ca; temperature 5° C; holding potential -70 mV throughout. Q_{max} estimated as 2400 $e/\mu m^2$. The curve represents the value of

$$\exp\left(\frac{V_p-19}{18}\right)\Big/\left(1+\exp\left(\frac{V_p-19}{18}\right)\right).$$

in rather few of the experiments were enough measurements made for the applicability of eqn. (4) to be tested at all severely. However, Fig. 19 shows that on the occasion when the most extensive set of values was obtained for the steady-state distribution of the mobile charges as a function of membrane potential, they fitted reasonably well with eqn. (5) when V' was taken as $+19$ mV and $kT/z'e$ as -18 mV. This provides some justification for the assumption made in writing eqn. (3) that when the charges make the transition from one side of the membrane to the other, their energy changes linearly with the potential difference.

Accepting that this treatment provides a satisfactory description of the steady-state properties of the system, its kinetics must next be considered.

If α is the forward rate constant or the probability of a transition from outside ('closed' condition of gate) to inside ('open'), and β is the probability of a transition back again, the differential equation governing the movement of the charges is

$$\frac{dN_1}{dt} = \alpha N_2 - \beta N_1$$

or
$$\frac{dp}{dt} = \alpha(1-p) - \beta p; \tag{10}$$

writing
$$\tau = \frac{1}{\alpha+\beta},$$

then
$$\frac{dp}{dt} = \alpha - \frac{p}{\tau}. \tag{11}$$

If $p = p_0$ at $t = 0$, and $p = p_V$ at $t = \infty$, the solution is

$$p = \alpha\tau + (p_0 - \alpha\tau)\, e^{-t/\tau}$$

or
$$p = p_V + (p_0 - p_V)\, e^{-t/\tau}. \tag{12}$$

The displacement current I_D is simply $Q_{max} . dp/dt$, so that its time course is given by

$$I_D = Q_{max} . \frac{1}{\tau}(p_V - p_0)\, e^{-t/\tau}. \tag{13}$$

Thus from large holding potentials where p_0 is negligibly small

$$I_D = Q_{max} . \alpha . e^{-t/\tau}. \tag{14}$$

Note that if p_0 cannot be neglected, there will be a reverse flow of displacement current during the hyperpolarizing pulse with a very short time constant τ', and the difference current actually recorded will be

$$I_D = Q_{max}\left\{\frac{1}{\tau}(p_V - p_0)e^{-t/\tau} - \frac{1}{\tau'} . p_0 . e^{-t/\tau'}\right\}. \tag{15}$$

Now in the steady state, the rates of transition forwards and backwards must always be equal, so that from (10)

$$\alpha(1-p_V) = \beta p_V, \tag{16}$$

and from (4)
$$\frac{\alpha}{\beta} = \frac{p_V}{1-p_V} = \exp\left[\frac{-z'e}{kT}(V - V')\right]. \tag{17}$$

For a single energy barrier (Rice, 1967), the rate constants α and β should vary exponentially with the energy difference, that is to say with membrane potential. Assuming in the first instance that a simple symmetry applies, eqn. (17) can best be satisfied by writing

$$\alpha = A \exp\left[\frac{-z'e}{2kT}(V - V')\right]$$

and $$\beta = \mathrm{A} \exp\left[\frac{z'e}{2kT}(V - V')\right],$$

where A is an unknown function of temperature and perhaps other variables. The time constant τ will then follow a symmetrical bell-shaped curve whose maximum, reached when $V = V'$, will be

$$\tau_{\max} = \frac{1}{2A}.$$

Hence $$\tau = \frac{2\tau_{\max}}{\exp\left[\frac{-z'e}{2kT}(V - V')\right] + \exp\left[\frac{z'e}{2kT}(V - V')\right]}. \tag{18}$$

As may be seen in Figs. 7, 16 and 20, eqn. (18) agreed only tolerably well with the experimental data for the dependence of τ on potential, but there is too much scatter of the individual values for the goodness of fit to be tested very critically. An important point to decide is whether, as has been assumed in deriving eqn. (18), the rate constants α and β are truly symmetrical functions of V. One way of examining this question is to calculate from the data in Table 3 the potential at which τ_{on} equals τ_{off}, and hence, knowing the holding potential, to estimate the position of the midpoint of a symmetrical curve passing through these two points, for comparison with the transition potential V' determined from the steady-state distribution of the charges. A difficulty is immediately introduced by the tendency of τ_{off} to increase with pulse size and duration. Taking only the values of τ_{off} for the smallest pulses, the estimated mid points agree to within a few mV with V', but in every case but one are more negative. If instead the largest values of τ_{off} are used for the calculation, the discrepancy is greater, the mid point being on average displaced 12 mV to the negative side of V'. It therefore seems that τ actually decreases more steeply with V on the positive side of V' than it does on the negative side, as is confirmed by an inspection of Fig. 20. It is not hard to think of reasons to explain such behaviour, among them being the probability that the charged particles encounter more than one energy barrier in making their transition across the membrane, and that they do not, as has tacitly been assumed, move independently of one another, but interact in some way.

In Fig. 20 we have assembled all the values of τ listed in Table 3, and have normalized them so that they are directly comparable with Hodgkin & Huxley's (1952) figures for τ_m. For this purpose we have taken the same standard temperature (= 6·3° C) and Q_{10} (= 3) as they did, and have allowed for an 18 mV shift along the voltage axis for the three axons perfused with 55 mM-CsF, since from the steady-state distribution of charges they had $V' = -4$ mV as compared with an average of $-21{\cdot}5$ mV

for the four intact axons. Chandler *et al.* (1965) found a shift of 22 mV in axons perfused with 50 mM-KCl. Except at large negative potentials beyond the normal resting potential, the agreement in magnitude between our data and the empirical curve (Hodgkin & Huxley, 1952, eqns. (20) and (21)) describing theirs is remarkably good; and the range where it is not is in fact that for which they had very few experimental results. Assuming that the average resting potential of their axons was close to -60 mV,

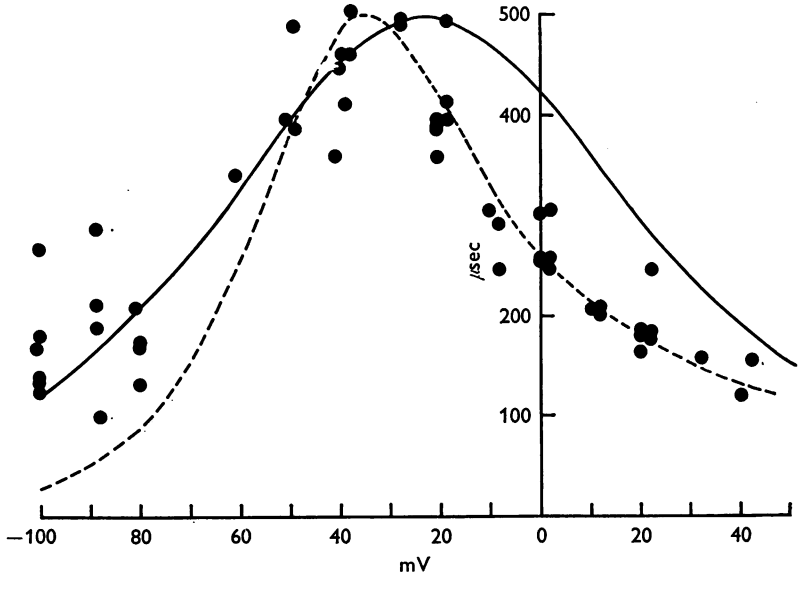

Fig. 20. Figures for the time constant taken from Table 3 and plotted against membrane potential after scaling to a standard temperature of 6·3° C and allowing for the voltage shift due to low internal ionic strength. The Q_{10} was taken as 3. Values of potentials for axons perfused with 55 mM-CsF were altered by -18 mV. The continuous line is drawn according to eqn. (18) with $\tau_{max} = 500$ μsec, $kT/z'e = 19$ mV and $V' = -21{\cdot}5$ mV. The dashed line is the value of τ_m at 6·3° C calculated from Hodgkin & Huxley (1952, eqns. (20) and (21), resting potential taken as -62 mV).

there is apparently a discrepancy between the mid point of their curve relating m_∞ to potential, which fell at $-60+25 = -35$ mV, and our transition potential (V') of $-21{\cdot}5$ mV. But in view of the small number of observations that we made, and some residual uncertainty over the exact corrections to be applied for junction potentials, the difference may not be significant. The equality over an appreciable range of potentials between the time constant of the asymmetrical displacement current and that of the 'm' system, and between the shifts of the curves induced by low internal ionic strength and high external Ca, seems too good to be

merely a coincidence, and may be regarded as strong evidence that the bulk of the mobile charges whose movements we are recording are indeed the Na gating particles.

If this identification is correct, we have next to consider why the curve relating peak Na conductance to membrane potential should be so much steeper than our steady-state distribution curve. The most obvious explanation would be that a cooperative phenomenon is somehow involved, or following the suggestion of Hodgkin & Huxley (1952), that several particles have to make the transition before an ionic gate is opened. To put this argument on a quantitative basis, we shall take the change in potential that gives rise to an e-fold increase in g_{Na} as just over 6 mV (see Table 2). This is greater than the 4 mV of Hodgkin & Huxley (1952), perhaps because we succeeded in compensating more completely for the Schwann cell series resistance than they did. Subsequent checks of the slope of the Na conductance curve in which the error from incomplete compensation was minimized by reducing I_{Na}, either by working in low external Na or by partially blocking the Na channels with tetrodotoxin, confirmed that 6 mV was close to the right value. Since the steady-state distribution curves for the mobile charges had a mean slope of 19 mV for an e-fold change, the effective cooperation number was 19/6 = 3. It again seems unlikely to be a pure coincidence that Hodgkin & Huxley (1952) found that their data for the kinetics of the Na conductance change were fitted better by m^3 than by m^2 or m^4. The most straightforward interpretation of this result would be that each channel actually incorporates three gating particles as part of its structure, but it should not be forgotten that there may be more subtle ways in which the same degree of cooperativity might be achieved without invoking a strictly stoicheiometric relation between the channels and the mobile charges. Another reason for wondering whether the cooperative mechanism is quite as simple as has been supposed is that our measurements suggest that the time constant for switching off the Na conductance at the end of a depolarizing voltage-clamp pulse is roughly equal to τ_{off} for the displacement current, instead of being the predicted one-third of it. Thus an examination of Fig. 1 of Keynes & Rojas (1973) shows that the average value of τ_{off} in the four runs was 117 ± 10 μsec for the displacement current as compared with 110 ± 16 μsec for the Na conductance. The membrane was being repolarized to -100 mV, well beyond the range covered by Hodgkin & Huxley (1952), so that there is no real experimental conflict with their observations. Yet another unexplained feature of our results that may be relevant here is the dependence of τ_{off} on pulse size. Both these questions have interesting implications for the molecular mechanism of the Na conductance change, and deserve further exploration.

From Table 5, the average value of the total charge displacement at saturation, Q_{max}, was 1882 $e/\mu m^2$. If at every sodium channel there were three controlling particles each carrying an effective charge of 1·3 e, the total number of channels would be $1882/3{\cdot}9 = 483/\mu m^2$. This may seem a rather large figure when compared with recent estimates of the density of tetrodotoxin binding sites in small fibres, which are respectively 2·5, 16 and $27/\mu m^2$ in gar olfactory nerve, lobster leg nerve and rabbit vagus (Colquhoun, Henderson & Ritchie, 1972). However, it is consistent in order of magnitude with estimates of the high-affinity specific binding sites in squid axons based on studies of tetrodotoxin kinetics (Keynes & Rojas 1973; and in preparation). Taking the Na conductance as '120 mmho/cm^2, since this estimate of Hodgkin & Huxley (1952) agrees well with our usual figures for fresh axons, the conductance of a single channel would be 2·5 pmho. This is a lower value than that worked out by Hille (1970), but his calculations were based on the tacit assumption that the density of tetrodotoxin binding sites observed in small lobster fibres was also valid for their giant axons. If the evolution of nerves specialized for rapid conduction involves an increase in the packing of Na channels as well as an increase in fibre diameter, then the possession of a high density of Na channels might be a general characteristic of all giant axons.

As might be suspected from a visual estimate of the areas of the records traced in Fig. 4, the total displacement of mobile charges turns out to be a respectable fraction of the displacement of charge across the regular 1 μF/cm^2 capacitance of the membrane. The effective capacitance of the mobile charge system is of course $Q_{max}.dp/dV$. By differentiating eqn. (5) and putting $V = V'$, it can readily be shown that at the steepest point on the steady-state distribution curve $dp/dV = -z'e/4kT$. Taking Q_{max} as $1882\ e/\mu m^2 = 3 \times 10^{-8}$ C/cm^2, and $-kT/z'e$ as 19 mV, the effective capacitance at the transition potential V' is found to be 0·4 μF/cm^2. Remembering that at 6° C the peak time constant for displacement of mobile charge is about 500 μsec, this means that the membrane should behave as though it has a large frequency and potential-dependent anomalous capacity exhibiting its maximum at a steady membrane potential in the neighbourhood of -20 mV and a frequency of 2 kc/s.

An obvious question is whether any of the asymmetrical displacement current can be attributed to the movements of Na-inactivating 'h' particles or K-inactivating 'n' particles. From eqn. (14) the initial current is seen to be proportional both to the forward rate constant and to the total charge displacement. The latter might well be much the same for 'h' and 'm', since the steepness of the h_∞ curve (Hodgkin & Huxley, 1952) suggests that the extra charge carried by the 'h' particles should just about compensate for their smaller number. For 'n' there is as yet no way of counting

the K channels, and it can only be assumed that they are roughly as numerous as the Na channels. The argument hinges, then, on the estimated sizes of the rate constants. According to Hodgkin & Huxley (1952), the forward rate constant for the '*h*' process, β_h in their notation, reaches a plateau value of 1 msec^{-1} for large depolarizations, while α_m is around 4 msec^{-1} when the membrane potential is taken to 0 mV. At this potential the initial value of $I_{D,h}$ would accordingly be about quarter of $I_{D,m}$. Such a substantial contribution from '*h*' has not so far been seen in any of our experiments, but measurements have not been made under conditions specifically chosen to unmask $I_{D,h}$ if it is present. This is a most important point for further examination, which may help to establish whether the concept of the '*h*' particles as separate entities is correct, or whether inactivation must rather be regarded as involving a second stage of interaction of the '*m*' particles after they have reached their activating positions and opened the gates. Similarly, no contribution to the displacement current from the '*n*' particles has yet been identified unequivocally, perhaps because α_n is always appreciably smaller than α_m. It may also be that the delayed rise in g_K seen at large holding potentials (see p. 411) means that the value of dn/dt at $t = 0$ is less than would be calculated from Hodgkin & Huxley's (1952) eqn. (7).

Another likely source of asymmetry in the displacement current that deserves consideration is the electrostriction effect. If there were a compression of the membrane by the electric field, and hence an increase in its capacity, that was symmetrical about zero membrane potential, then under the conditions of our measurements the capacity transient for the hyperpolarizing pulse would be slightly larger than that for the depolarizing pulse, and the difference would appear as an inward current. The electrostriction signal would therefore be in the opposite direction to those that we actually observe. Even if the electrostriction effect were increased in size by displacement of the potential for maximum thickness of the membrane towards a more positive value as in Fig. 8 of Cohen, Hille, Keynes, Landowne & Rojas (1971) for the fast retardation change, with which it may possibly be identified, it would still be relatively insignificant in absolute magnitude. As Cohen *et al.* (1971) pointed out, the fractional change in membrane thickness for a 50 mV pulse is probably of the order of 0·1 %. The electrostriction effect will not be easy to detect under any circumstances.

We are indebted to the Royal Society and to the Underwood Fund of the A.R.C. for grants to E.R., to Mr S. B. Cross for his unfailing assistance with many aspects of this work, and to Professor Sir Alan Hodgkin for valuable discussion.

REFERENCES

ARMSTRONG, C. M. (1974). Ionic pores, gates, and gating currents. *Q. Rev. Biophys.* **6** (in the Press).

ARMSTRONG, C. M. & BEZANILLA, F. (1973). Currents related to movement of the gating particles of the sodium channels. *Nature, Lond.* **242**, 459–461.

BEZANILLA, F., ROJAS, E. & TAYLOR, R. E. (1970). Sodium and potassium conductance changes during a membrane action potential. *J. Physiol.* **211**, 729–751.

CHANDLER, W. K., HODGKIN, A. L. & MEVES, H. (1965). The effect of changing the internal solution on sodium inactivation and related phenomena in giant axons. *J. Physiol.* **180**, 821–836.

CHANDLER, W. K. & MEVES, H. (1965). Voltage clamp experiments on internally perfused giant axons. *J. Physiol.* **180**, 788–820.

CHANDLER, W. K. & MEVES, H. (1970*a*). Sodium and potassium currents in squid axons perfused with fluoride solutions. *J. Physiol.* **211**, 623–652.

CHANDLER, W. K. & MEVES, H. (1970*b*). Evidence for two types of sodium conductance in axons perfused with sodium fluoride solutions. *J. Physiol.* **211**, 653–678.

COHEN, L. B., HILLE, B., KEYNES, R. D., LANDOWNE, D. & ROJAS, E. (1971). Analysis of the potential-dependent changes in optical retardation in the squid giant axon. *J. Physiol.* **218**, 205–237.

COLE, K. S. & MOORE, J. W. (1960). Potassium ion current in the squid giant axon: dynamic characteristics. *Biophys. J.* **1**, 1–14.

COLQUHOUN, D., HENDERSON, R. & RITCHIE, J. M. (1972). The binding of labelled tetrodotoxin to non-myelinated nerve fibres. *J. Physiol.* **227**, 95–126.

FRANKENHAEUSER, B. & HODGKIN, A. L. (1957). The action of calcium on the electrical properties of squid axons. *J. Physiol.* **137**, 218–244.

HILLE, B. (1970). Ionic channels in nerve membranes. *Progr. Biophys. molec. Biol.* **21**, 3–32.

HODGKIN, A. L. & HUXLEY, A. F. (1952). A quantitative description of membrane current and its application to conduction and excitation in nerve. *J. Physiol.* **117**, 500–544.

KEYNES, R. D. & ROJAS, E. (1973). Characteristics of the sodium gating current in the squid giant axon. *J. Physiol.* **233**, 28–30*P*.

MOORE, J. W. & COLE, K. S. (1963). Voltage clamp technique. In *Physical Techniques in Biological Research*, vol. VI, *Electrophysiological Methods*, part B, ed. NASTUK, W. L. New York: Academic Press.

MOORE, J. W., NARAHASHI, T. & SHAW, T. I. (1967). An upper limit to the number of sodium channels in nerve membrane? *J. Physiol.* **188**, 99–105.

RICE, O. K. (1967). *Statistical Mechanics, Thermodynamics and Kinetics.* San Francisco: Freeman.

ROJAS, E., TAYLOR, R. E., ATWATER, I. & BEZANILLA, F. (1969). Analysis of the effects of calcium or magnesium on voltage-clamp currents in perfused squid axons bathed in solutions of high potassium. *J. gen. Physiol.* **54**, 532–552.

SEEMAN, P. (1972). The membrane actions of anaesthetics and tranquilizers. *Pharmac. Rev.* **24**, 583–655.

TAYLOR, R. E. (1959). Effect of procaine on electrical properties of squid axon membrane. *Am. J. Physiol.* **196**, 1071–1078.